Chiueh C. C., Andoh T. and Chock P. B. (2005) Induction of thioredoxin and mitochondrial survival proteins mediates preconditioning-induced cardioprotection and neuroprotection. *Ann. NY Acad. Sci.* **1042**, 403–418.

Choi W. S., Eom D. S., Han B. S., Kim W. K., Han B. H., Choi E. J., Oh T. H., Markelonis G. J., Cho J. W. and Oh Y. J. (2004) Phosphorylation of p38 MAPK induced by oxidative stress is linked to activation of both caspase-8- and -9-mediated apoptotic pathways in dopaminergic neurons. *J. Biol. Chem.* **279**, 20 451–20 460.

Coyle J. T. and Puttfarcken P. (1993) Oxidative stress, glutamate, and neurodegenerative disorders. *Science* **262**, 689–695.

Das K. C. and Das C. K. (2000) Thioredoxin, a singlet oxygen quencher and hydroxyl radical scavenger: redox independent functions. *Biochem. Biophys. Res. Commun.* **277**, 443–447.

El-Remessy A. B., Khalil I. E., Matragoon S., Abou-Mohamed G., Tsai N. J., Roon P., Caldwell R. B., Caldwell R. W., Green K. and Liou G. I. (2003) Neuroprotective effect of (-)Delta9-tetrahydrocannabinol and cannabidiol in *N*-methyl-D-aspartate-induced retinal neurotoxicity: involvement of peroxynitrite. *Am. J. Pathol.* **163**, 1997–2008.

Filomeni G., Rotilio G. and Ciriolo M. R. (2003) Glutathione disulfide induces apoptosis in U937 cells by a redox-mediated p38 MAP kinase pathway. *FASEB J.* **17**, 64–66.

Hansson H. A., Holmgren A., Norstedt G. and Rozell B. (1989) Changes in the distribution of insulin-like growth factor I, thioredoxin, thioredoxin reductase and ribonucleotide reductase during the development of the retina. *Exp. Eye Res.* **48**, 411–420.

Hartwick A. T., Lalonde M. R., Barnes S. and Baldridge W. H. (2004) Adenosine A1-receptor modulation of glutamate-induced calcium influx in rat retinal ganglion cells. *Invest. Ophthalmol. Vis. Sci.* **45**, 3740–3748.

Hattori I., Takagi Y., Nakamura H., Nozaki K., Bai J., Kondo N., Sugino T., Nishimura M., Hashimoto N. and Yodoi J. (2004) Intravenous administration of thioredoxin decreases brain damage following transient focal cerebral ischemia in mice. *Antioxid. Redox Signal* **6**, 81–87.

Herin G. A. and Aizenman E. (2004) Amino terminal domain regulation of NMDA receptor function. *Eur. J. Pharmacol.* **500**, 101–111.

Holmgren A. (1985) Thioredoxin. *Annu. Rev. Biochem.* **54**, 237–271.

Ichiki H., Hoshino T., Kinoshita T., Imaoka H., Kato S., Inoue H., Nakamura H., Yodoi J., Young H. A. and Aizawa H. (2005) Thioredoxin suppresses airway hyperresponsiveness and airway inflammation in asthma. *Biochem. Biophys. Res. Commun.* **334**, 1141–1148.

Inomata Y., Hirata A., Yonemura N., Koga T., Kido N. and Tanihara H. (2003a) Neuroprotective effects of interleukin-6 on NMDA-induced rat retinal damage. *Biochem. Biophys. Res. Commun.* **302**, 226–232.

Inomata Y., Hirata A., Koga T., Kimura A., Singh D. P., Shinohara T. and Tanihara H. (2003b) Lens epithelium-derived growth factor: neuroprotection on rat retinal damage induced by *N*-methyl-D-aspartate. *Brain Res.* **991**, 163–170.

Kondo N., Ishii Y., Kwon Y. W., Tanito M., Horita H., Nishinaka Y., Nakamura H. and Yodoi J. (2004) Redox-sensing release of human thioredoxin from T lymphocytes with negative feedback loops. *J. Immunol.* **172**, 442–448.

Lam T. T., Abler A. S., Kwong J. M. and Tso M. O. (1999) *N*-methyl-D-aspartate (NMDA)-induced apoptosis in rat retina. *Invest. Ophthalmol. Vis. Sci.* **40**, 2391–2397.

Levin L. A. and Louhab A. (1996) Apoptosis of retinal ganglion cells in anterior ischemic optic neuropathy. *Arch. Ophthalmol.* **114**, 488–491.

Levy D. I., Sucher N. J. and Lipton S. A. (1991) Glutathione prevents N-methyl-D-aspartate receptor-mediated neurotoxicity. *Neuroreport* **2**, 345–347.

Lipton S. A., Choi Y. B., Takahashi H., Zhang D., Li W., Godzik A. and Bankston L. A. (2002) Cysteine regulation of protein function – as exemplified by NMDA-receptor modulation. *Trends Neurosci.* **25**, 474–480.

Liu W., Nakamura H., Shioji K., Tanito M., Oka S., Ahsan M. K., Son A., Ishii Y., Kishimoto C. and Yodoi J. (2004) Thioredoxin-1 ameliorates myosin-induced autoimmune myocarditis by suppressing chemokine expressions and leukocyte chemotaxis in mice. *Circulation* **110**, 1276–1283.

Manabe S. and Lipton S. A. (2003) Divergent NMDA signals leading to proapoptotic and antiapoptotic pathways in the rat retina. *Invest. Ophthalmol. Vis. Sci.* **44**, 385–392.

Masutani H., Ueda S. and Yodoi J. (2005) The thioredoxin system in retroviral infection and apoptosis. *Cell Death Differ.* **12**, 991–998.

Mielke K. and Herdegen T. (2000) JNK and p38 stresskinases — degenerative effectors of signal-transduction-cascades in the nervous system. *Prog. Neurobiol.* **61**, 45–60.

Mitsui A., Hirakawa T. and Yodoi J. (1992) Reactive oxygen-reducing and protein-refolding activities of adult T cell leukemia-derived factor/human thioredoxin. *Biochem. Biophys. Res. Commun.* **186**, 1220–1226.

Munemasa Y., Ohtani-Kaneko R., Kitaoka Y. *et al.* (2005) Contribution of mitogen-activated protein kinases to NMDA-induced neurotoxicity in the rat retina. *Brain Res.* **1044**, 227–240.

Murphy T. H., Miyamoto M., Sastre A., Schnaar R. L. and Coyle J. T. (1989) Glutamate toxicity in a neuronal cell line involves inhibition of cystine transport leading to oxidative stress. *Neuron* **2**, 1547–1558.

Nakamura H., Nakamura K. and Yodoi J. (1997) Redox regulation of cellular activation. *Annu. Rev. Immunol.* **15**, 351–369.

Nakamura H., Herzenberg L. A., Bai J., Araya S., Kondo N., Nishinaka Y., Herzenberg L. A. and Yodoi J. (2001) Circulating thioredoxin suppresses lipopolysaccharide-induced neutrophil chemotaxis. *Proc. Natl Acad. Sci. USA* **98**, 15 143–15 148.

Rosenbaum D. M., Rosenbaum P. S., Gupta H., Singh M., Aggarwal A., Hall D. H., Roth S. and Kessler J. A. (1998) The role of the p53 protein in the selective vulnerability of the inner retina to transient ischemia. *Invest. Ophthalmol. Vis. Sci.* **39**, 2132–2139.

Saitoh M., Nishitoh H., Fujii M., Takeda K., Tobiume K., Sawada Y., Kawabata M., Miyazono K. and Ichijo H. (1998) Mammalian thioredoxin is a direct inhibitor of apoptosis signal-regulating kinase (ASK) 1. *EMBO J.* **17**, 2596–2606.

Schori H., Kipnis J., Yoles E., WoldeMussie E., Ruiz G., Wheeler L. A. and Schwartz M. (2001) Vaccination for protection of retinal ganglion cells against death from glutamate cytotoxicity and ocular hypertension: implications for glaucoma. *Proc. Natl Acad. Sci. USA* **98**, 3398–3403.

Schwarcz R. and Coyle J. T. (1977) Kainic acid: neurotoxic effects after intraocular injection. *Invest. Ophthalmol. Vis. Sci.* **16**, 141–148.

Shibuki H., Katai N., Kuroiwa S., Kurokawa T., Yodoi J. and Yoshimura N. (1998) Protective effect of adult T-cell leukemia-derived factor on retinal ischemia-reperfusion injury in the rat. *Invest. Ophthalmol. Vis. Sci.* **39**, 1470–1477.

Siliprandi R., Canella R., Carmignoto G., Schiavo N., Zanellato A., Zanoni R. and Vantini G. (1992) *N*-methyl-D-aspartate-induced neurotoxicity in the adult rat retina. *Vis. Neurosci.* **8**, 567–573.

Sucher N. J., Lipton S. A. and Dreyer E. B. (1997) Molecular basis of glutamate toxicity in retinal ganglion cells. *Vision Res.* **37**, 3483–3493.

Tagaya Y., Maeda Y., Mitsui A. *et al.* (1989) ATL-derived factor (ADF), an IL-2 receptor/Tac inducer homologous to thioredoxin; possible involvement of dithiol-reduction in the IL-2 receptor induction. *EMBO J.* **8**, 757–764.

Takagi Y., Mitsui A., Nishiyama A., Nozaki K., Sono H., Gon Y., Hashimoto N. and Yodoi J. (1999) Overexpression of thioredoxin in transgenic mice attenuates focal ischemic brain damage. *Proc. Natl Acad. Sci.* **96**, 4131–4134.

Tanaka T., Hosoi F., Yamaguchi-Iwai Y. *et al.* (2002) Thioredoxin-2 (TRX-2) is an essential gene regulating mitochondria-dependent apoptosis. *EMBO J.* **21**, 1695–1703.

Tanito M., Masutani H., Nakamura H., Ohira A. and Yodoi J. (2002a) Cytoprotective effect of thioredoxin against retinal photic injury in mice. *Invest. Ophthalmol. Vis. Sci.* **43**, 1162–1167.

Tanito M., Masutani H., Nakamura H., Oka S., Ohira A. and Yodoi J. (2002b) Attenuation of retinal photooxidative damage in thioredoxin transgenic mice. *Neurosci. Lett.* **326**, 142–146.

Tanito M., Nishiyama A., Tanaka T., Masutani H., Nakamura H., Yodoi J. and Ohira A. (2002c) Change of redox status and modulation by thiol replenishment in retinal photooxidative damage. *Invest. Ophthalmol. Vis. Sci.* **43**, 2392–2400.

Tanito M., Masutani H., Kim Y. C., Nishikawa M., Ohira A. and Yodoi J. (2005a) Sulforaphane induces thioredoxin through the antioxidant-responsive element and attenuates retinal light damage in mice. *Invest. Ophthalmol. Vis. Sci.* **46**, 979–987.

Tanito M., Kwon Y. W., Kondo N., Bai J., Masutani H., Nakamura H., Fujii J., Ohira A. and Yodoi J. (2005b) Cytoprotective effects of geranylgeranylacetone against retinal photooxidative damage. *J. Neurosci.* **25**, 2396–2404.

Thoreson W. B. and Witkovsky P. (1999) Glutamate receptors and circuits in the vertebrate retina. *Prog. Retin. Eye Res.* **18**, 765–810.

Ueda S., Nakamura H., Masutani H., Sasada T., Yonehara S., Takabayashi A., Yamaoka Y. and Yodoi J. (1998) Redox regulation of caspase-3(-like) protease activity: regulatory roles of thioredoxin and cytochrome c. *J. Immunol.* **161**, 6689–6695.

Ueda S., Masutani H., Nakamura H., Tanaka T., Ueno M. and Yodoi J. (2002) Redox control of cell death. *Antioxid. Redox Signal* **4**, 405–414.

Wehrwein E., Thompson S. A., Coulibaly S. F., Linn D. M. and Linn C. L. (2004) Acetylcholine protection of adult pig retinal ganglion cells from glutamate-induced excitotoxicity. *Invest. Ophthalmol. Vis. Sci.* **45**, 1531–1543.

Yodoi J. and Uchiyama T. (1992) Diseases associated with HTLV-I: virus, IL-2 receptor dysregulation and redox regulation. *Immunol. Today* **13**, 405–411.

Molecular Vision 2006; 12:977-82 <http://www.molvis.org/molvis/v12/a109/>
Received 22 December 2005 | Accepted 16 June 2006 | Published 17 August 2006

Elevated neprilysin activity in vitreous of patients with proliferative diabetic retinopathy

Hideaki Hara,[1] Kentaro Oh-hashi,[2] Shinji Yoneda,[3] Masamitsu Shimazawa,[1] Masaru Inatani,[4] Hidenobu Tanihara,[4] Kazutoshi Kiuchi[2]

[1]Department of Biofunctional Molecules, Gifu Pharmaceutical University, 5-6-1 Mitahora-higashi, Gifu, [2]Department of Biomolecular Science, Faculty of Engineering, Gifu University, 1-1 Yanagido, Gifu, [3]Research and Development Center, Santen Pharmaceutical Co. Ltd., 8916-16 Takayama-cho, Ikoma, [4]Department of Ophthalmology and Visual Science, Kumamoto University Graduate School of Medical Sciences, 1-1-1 Honjo, Kumamoto, Japan

Purpose: Diabetic retinopathy (DR) is the leading cause of blindness in the industrialized world. Hyperglycemia induces retinal hypoxia, which upregulates a range of vasoactive factors that may lead to macular edema and/or angiogenesis, and hence potentially to sight-threatening retinopathy. The control of signal-peptide activity by cell-surface proteases is one of the main factors regulating the development and behavior of organisms. In mammals, neprilysin is known to play a key role in these processes, and its inactivation can initiate cellular disorganization. Neprilysin is a rate-limiting peptidase involved in the physiological degradation of amyloid β (Aβ) in the brain. In this study, we measured both the enzymatic activity of neprilysin and the concentration of Aβ in patients with proliferative DR (as compared to their levels in patients with macular hole), and we analyzed their association.

Methods: In vitreous samples collected from patients who underwent vitrectomy, an HPLC-fluorometric system (recently established by us), and sensitive and specific enzyme-linked immunosorbent assays were used to determine the enzymatic activity of neprilysin and the concentration of Aβ.

Results: By comparison with the levels in the control (macular-hole) patients, there was a significant increase in neprilysin activity level and a significant decrease in Aβ level in proliferative DR patients. There was a significant inverse correlation between neprilysin and Aβ among all subjects.

Conclusions: Neprilysin activity and Aβ concentrations displayed converse changes in patients with proliferative DR.

Diabetic retinopathy (DR) is the leading cause of acquired blindness among young adults, and studies have shown that it is the hyperglycemia itself that initiates its development [1]. In the pathogenesis of retinopathy in diabetes, certain cells (retinal microvascular endothelial, Müller, and ganglion cells and pericytes) are lost selectively via apoptosis before any other histopathology is detectable and before any loss of vision is evident [2,3].

Alzheimer's disease (AD) is characterized by the accumulation of amyloid β peptide (Aβ) in the brain. Aβ is constitutively produced by proteolysis of β-amyloid precursor protein (APP) [4,5]. The pathological formation of amyloid plaques is thought to be the primary force driving the pathogenesis of Alzheimer's disease. Hence, much attention has been focused on the production of Aβ. Neprilysin (variously known as neutrophil cluster-differentiation antigen 10 (CD10), neuronal endopeptidase 24-11, or enkephalinase) is considered the most important enzyme for Aβ degradation in the brain [6,7]. Recently, genetic approaches using neprilysin-deficient mice have demonstrated the ability of neprilysin to cleave endogenous Aβ [8,9]. Moreover, a decline in neprilysin levels has been found in the brain in patients with early-stage sporadic AD [10], suggesting critical roles for reduced neprilysin activity in the incipient process of Aβ accumulation.

The prevalence of both Alzheimer disease and type 2 diabetes increases with age, and both have genetic components [11-16], raising the possibilitity that patients with Alzheimer disease may be more vulnerable to type 2 diabetes and raising the possibility of a linkage between the processes responsible for the loss of brain cells and the loss of β-cells in these diseases [17]. It has been reported that diabetes-related mitochondrial dysfunction is exacerbated by aging and/or by the presence or neurotoxic agents, such as Aβ, suggesting that diabetes and aging are risk factors for the neurodegeneration induced by these peptides [18]. Taken together, these data indicate that a correlation may exist among the age-related pathologies diabetes and AD. We have reported changes in the levels of Alzheimer's disease-related factors (such as Aβ and Tau) in vitreous bodies obtained from patients with DR, indicating that Aβ42 and Tau may be implicated in the pathogenesis of DR and that the neurodegeneration processes of DR may share, at least in part, common mechanism with Alzheimer's disease [19]. However, the detailed mechanisms are unclear at this time. Hence, the purpose of the present study was to determine the vitreous concentrations of neprilysin and Aβ in proliferative DR and to analyze the relationship between neprilysin and Aβ.

Correspondence to: Dr. Hideaki Hara, PhD, Department of Biofunctional Molecules, Gifu Pharmaceutical University, 1-5-90 Mitahora-higashi, Gifu 502-8585, Japan; Phone: +81-58-237-3931; FAX: +81-58-237-5979; email: hidehara@gifu-pu.ac.jp

METHODS

Sampling from patients: This study was conducted according to the tenets of the Declaration of Helsinki. Informed consent was obtained from all patients who underwent vitrectomy, and the study was carried out in accordance with the guidelines of the human studies committee of Kumamoto University. Patient diagnoses were idiopathic macular hole and proliferative DR (Table 1). Samples obtained from patients with a vitreous hemorrhage were not included in this study. The control group was made up of samples from eight eyes in eight patients with macular hole. Vitreous samples were also collected from ten eyes in ten patients with proliferative DR.

Measurement of neprilysin activity: Dansyl-D-Ala-Gly-p-nitro-Phe-Gly [20], Dansyl-D-Ala-Gly and thiorphan [21,22] were purchased from Sigma (st. Loius, MO). Recombinant human neprilysin was obtained from R&D Systems (Minneapolis, MN). Measurement of neprilysin activity was performed according to our previous report [23], with some modifications. In brief, 5 ml of vitreous fluid was added to 50 µl of 20 mM HEPES buffer (pH 7.2) containing a fluorescent substrate, Dansyl-D-Ala-Gly-p-nitro-Phe-Gly (200 µM), in the presence or absence of thiorphan (50 mM). Then, each sample was incubated for 60 min at 37 °C. After incubation for 5 min at 90 °C and centrifugation at 15,000 rpm for 5 min, an aliquot of the supernatant (10 µl) was used for HPLC analysis. The Dansyl-D-Ala-Gly produced from the fluorescent substrate was measured fluorometrically using an HPLC apparatus (Shimazu, RF10AXL). A reverse-phase gel column (i.e., an Inertosil-3 C18 column; 4.6 mm Φ 400 mm; GL Science) with a guard column was used for the assay. The sample was eluted using 40% (v/v) acetonitrile containing 0.05% trifluoroacetic acid at a flow rate of 0.5 ml/min at 40 °C. The amount of product was estimated by measuring its fluorescence intensity at 562 nm, with excitation at 342 nm. Protease activity (pmol/h/ml) in the vitreous fluid was estimated from the standard curve of synthetic Dansyl-D-Ala-Gly fluorescence intensity. Neprilysin-like activity (thiorphan-sensitive peptidase activity) in each sample was evaluated by subtraction of thiorphan-insensitive enzymatic activity (i.e., that recorded in the presence of thiorphan) from total activity.

Measurement of amyloid β: Specimens were collected in sterile tubes and stored at -80 °C until the analysis was conducted. Sensitive, specific enzyme-linked immunosorbent assays (ELISA) specific for Aβ42 were used for the analysis (INNOTEST β-amyloid$_{(1-42)}$; Innogenetics, Gent, Belgium). Six out of eight vitreous samples in the proliferative DR group were used to measure Aβ$_{42}$, because the volume of two samples was insufficient for measurement purposes. All samples were run in duplicate. The experiment was carried out in a masked fashion (by SY).

Statistical analysis: Data are expressed as means±SEM and were analyzed using a one-way ANOVA followed by a Student t-test.

Table 1. Clinical characteristics of patients

Name	Control (macular hole)	Proliferative diabetic retinopathy
n (Total)	8	10
Male	4	6
Female	4	4
Age	66.9 ± 3.1	52.2 ± 3.4

Clinical characteristics of patients with macular hole and proliferative diabetic retinopathy. Age is mean±SEM in years.

RESULTS

Neprilysin-like activity in vitreous of patients with proliferative diabetic retinopathy: The clinical characteristics of the patients providing vitreous fluid data are given in Table 1. Figure 1 shows the neprilysin-like activity levels in the vitreous of patients with macular hole (Control) or proliferative DR (Patient), with representative chromatograms for the measurement of neprilysin activity being shown in Figure 1A. The values for peptidase activity, obtained using Dansyl-D-Ala-Gly-p-nitro-Phe-Gly, in the Control group (n=8) were 0.92±0.03 and 0.77±0.04 pmol/h/µl (mean±SEM) in the absence and presence of thiorphan, respectively. In the Patient (n=10) group, the corresponding values were 1.45±0.14 and 0.75±0.03 pmol/h/µl in the absence and presence of thiorphan, respectively. There was a significant difference between the Control and Patient groups in total activity (without thiorphan), whereas the thiorphan-insensitive activities of the two groups were almost the same (Figure 1B). The values obtained for neprilysin-like peptidase activity in Control (n=8) and Patient (n=10) groups were 0.15±0.03 and 0.70±0.12 pmol/h/µl, respectively, the mean value for patients with proliferative DR being approximately 4.7 times that of the controls (Figure 1C).

Concentration of amyloid β in vitreous of patients with proliferative diabetic retinopathy: Figure 2 shows the concentrations of Aβ in the vitreous of patients with macular hole (Control) or proliferative DR (Patient). In Control (n=6) and Patient (n=10) groups, these values were 60.9±7.34 and 8.94±3.30 pg/ml, respectively, the latter value being significantly smaller than the former.

Relationship between neprilysin-like activity and amyloid β concentration in vitreous: Figure 3 shows that neprilysin-like peptidase activity was elevated and, in contrast, the Aβ concentration was reduced in the vitreous of proliferative DR patients (versus the controls). There was a significant inverse correlation ($y=-0.0089x + 0.7472$, $p=0.0072$, $R^2=0.4134$) between neprilysin-like peptidase activity and Aβ concentration among all subjects.

DISCUSSION

In this study, we observed a significant increase in neprilysin-like peptidase activity and a significant reduction in Aβ concentration in the vitreous fluid of patients with proliferative DR (by comparison with macular hole patients), and a significant inverse correlation was revealed between these two parameters in vitreous fluid.

Recent reports [19,24-27] suggest that Aβ increases in various areas of the eye during the progression of eye diseases, and therefore that the increase in Aβ might contribute to the eye disease. Interestingly, Aβ deposition has been reported to be specific to drusen in the eyes of patients with age-related macular degeneration (AMD) [24-26], suggesting that Aβ might be associated with the more advanced stages of AMD [26]. AMD is a retinal degenerative disease that leads to a loss of central vision, and it affects 5-10% of the population over 60 years of age. A number of studies have confirmed that the presence of drusen-identified as gray-yellow deposits that collect in or around the macula of the retina-represents a significant risk factor for the development of visual loss from AMD [28-30]. Goldstein et al. [27] noted that Aβ is present in the cytosol of lens fiber cells in patients with AD and that the presence of Aβ in the lens might promote regionally specific lens protein aggregation, extracerebral amyloid formation and supranuclear cataracts. Recently, an association between diabetes mellitus and an increased risk of developing AD has been suggested (i.e., diabetes mellitus may be associated with the development of AD and with the decline in cognitive function in older persons) [31]. We reported recently that the concentrations of Aβ42 and tau showed a decrease and an increase, respectively (versus macular hole controls), in the vitreous fluid from patients with glaucoma and DR [19]. However, there have been no previous reports regarding changes in neprilysin in eye diseases.

An increase in TUNEL-positive cells in retinal neurons has been observed at an early stage in streptozotocin-diabetic rats and in human diabetes, and neurodegeneration may be an important component of DR [32]. Given our finding that a decrease in the concentration of Aβ42 in the vitreous fluid obtained from patients with DR is observed regardless of the manner of the disease progression (proliferative or edematous), it is possible that factors associated with the early stages of diabetes development may affect Aβ metabolism in the retina,

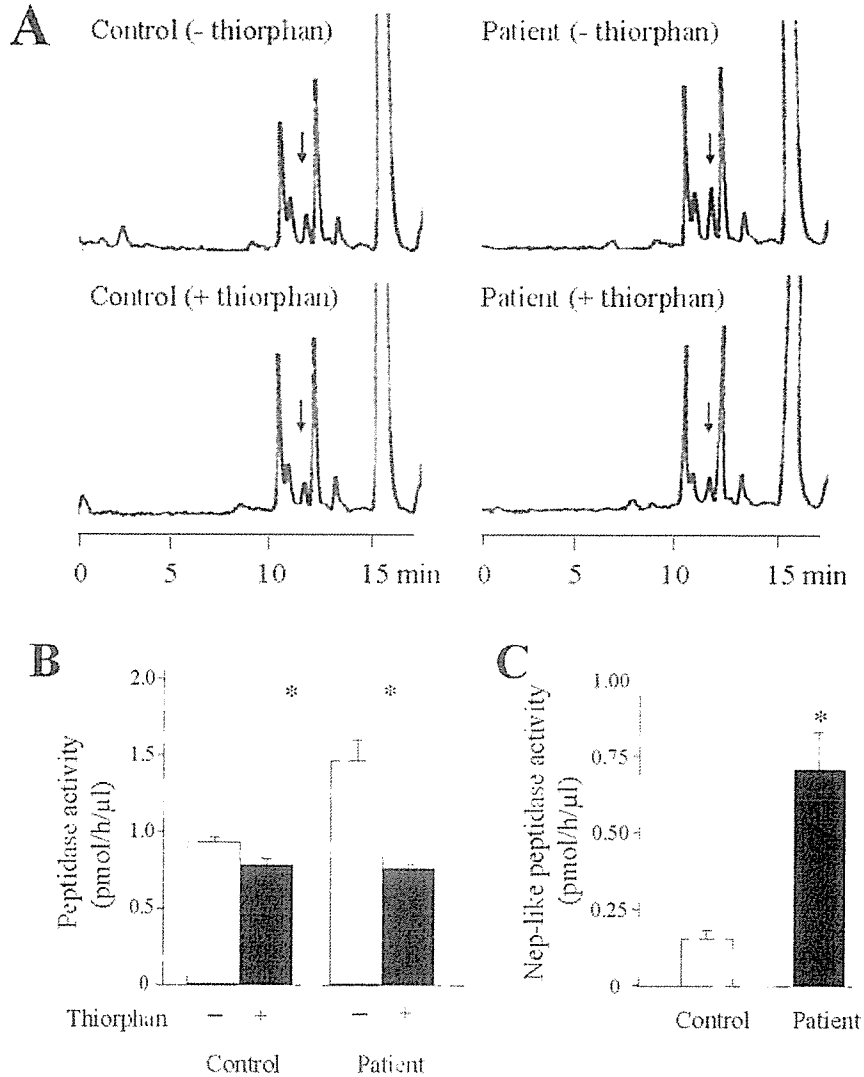

Figure 1. Neprilysin-like peptidase activity in vitreous samples. Neprilysin-like peptidase activity was measured in vitreous samples obtained from patients with macular hole (Control) or proliferative diabetic retinopathy (Patient). **A**: Representative chromatograms for measurement of neprilysin activity. Arrows indicate the product, Dansyl-D-Ala-Gly. **B**: Peptidase activity in the absence (open column) or presence (solid column) of thiorphan was measured by means of an HPLC-fluorometric system, as described under Materials and Methods. **C**: Neprilysin-like peptidase activity was calculated by subtraction of thiorphan-insensitive peptidase activity from total activity. Values are mean±SEM, n=8 (Control) and 10 (Patient). Asterisk (*) represents $p<0.001$ (Student t-test).

possibly leading to neurodegeneration in DR. Further studies will be needed for a full elucidation of the alterations in Aβ in DR.

Recently, we established a novel, sensitive protocol for the measurement of extracellular cell-surface neprilysin activity in living cells (using an HPLC apparatus) [23]. Using this system, we investigated the effect of hypoxia on neprilysin activity in human neuroblastoma SH-SY5Y cells, and we demonstrated that hypoxia (under 5% O_2 for 24 h)-an event closely associated with DR and neurodegenerative diseases-significantly attenuated neprilysin activity without any alteration in neprilysin gene expression [23]. Neprilysin is reported to be secreted from LLC-PK1 cells (originate from pig proximal tubule of the nephron) [33], human prostatic secretory cells [34] and invasive human melanoma cell lines [35]. In case of prostatic tissue, neprilysin is released from the cells in an apocrine fashion [34]. Recently, it was shown that cerebrospinal fluid (CSF) neprilysin elevates with the progression of Alzheimer's disease, and suggested that presynaptically located neprilysin could be released into CSF as a consequence of synaptic disruption [36]. Therefore, one possibility is that under a hypoxic condition, neprilysin is released from membrane, with the result that soluble neprilysin is increased at the extracellular level.

A limitation of the present study is the small sample sizes. Nevertheless, we observed an apparent relationship between increased neprilysin-like peptidase activity and decreased Aβ concentration in patients with proliferative DR. On the basis of the present data, we can speculate about the underlying mechanism as follows. One of many possible reasons for this observation is degradation of Aβ by neprilysin. Namely, retinal damage is induced by DR, and consequently the neprilysin bound to the membrane of the retinal cells is cleaved off, thereby increasing the concentration of soluble neprilysin within the vitreous body. If membrane-anchored neprilysin serves to offer a locus for the degradation of newly generated Aβ within the synapse, any neprilysin separated from the cell membrane will not be able to perform its role of scavenging synaptic Aβ molecules. It is possible that a decrease in cell-surface neprilysin causes an enhancement of Aβ aggregation within the synapse and a degeneration of ganglion cells within the retina. This hypothesis is consistent with the observation of a decrease in Aβ42 in the vitreous of patients with proliferative DR since some might form aggregates on the membrane of retinal cells, while others might be degraded by soluble neprilysin within the vitreous.

There are other possible mechanisms, as follows: in DR patients, Aβ accumulates the retina for some reason and consequently Aβ and neprilysin levels in the vitreous decrease and increase, respectively. Aβ is reportedly detected in retinal ganglion cells (by immunohistochemistry) significantly more often in ocular hypertensive retinas than in control retinas [37]. Further work will be necessary to determine whether the decrease in the Aβ level really is related to the increase in neprilysin activity.

In conclusion, neprilysin activity and Aβ concentrations displayed converse changes in patients with proliferative DR, there being a significant inverse correlation between the two parameters.

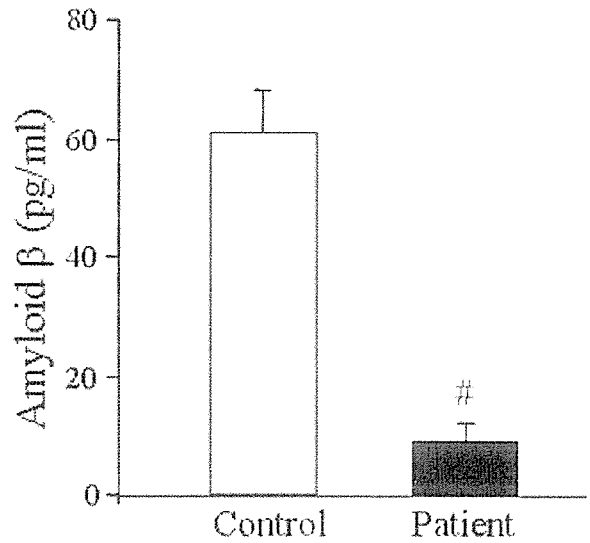

Figure 2. Concentrations of β-amyloid$_{(1-42)}$ (Aβ42) in vitreous samples. Aβ42 was measured in vitreous samples obtained from patients with macular hole (Control) or proliferative diabetic retinopathy (Patient) by use of sensitive, specific enzyme-linked immunosorbent assays (ELISA), as described under Methods. Values are mean±SEM, n=6 (Control) and 10 (Patient). Sharp (#) indicates p<0.0001 for comparison to control (Student t-test).

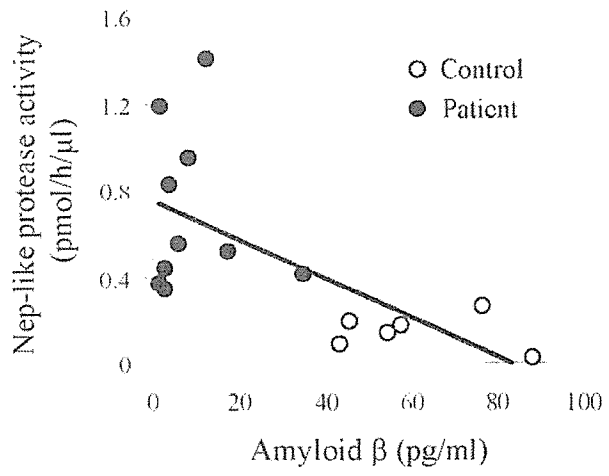

Figure 3. Relationship between neprilysin-like peptidase activity and amyloid β concentration in vitreous. Neprilysin-like peptidase activity was elevated and, in contrast, Aβ was reduced in the vitreous of proliferative DR patients (versus Control). There was a significant inverse correlation (y=-0.0089x + 0.7472, p=0.0072, R^2=0.4134) between neprilysin-like peptidase activity and Aβ among all subjects.

ACKNOWLEDGEMENTS

This study was supported by the Gifu Prefecture Research Foundation and the Naito Foundation.

REFERENCES

1. Engerman RL, Kern TS. Experimental galactosemia produces diabetic-like retinopathy. Diabetes 1984; 33:97-100.
2. Mizutani M, Kern TS, Lorenzi M. Accelerated death of retinal microvascular cells in human and experimental diabetic retinopathy. J Clin Invest 1996; 97:2883-90.
3. Kern TS, Tang J, Mizutani M, Kowluru RA, Nagaraj RH, Romeo G, Podesta F, Lorenzi M. Response of capillary cell death to aminoguanidine predicts the development of retinopathy: comparison of diabetes and galactosemia. Invest Ophthalmol Vis Sci 2000; 41:3972-8.
4. De Strooper B, Annaert W. Proteolytic processing and cell biological functions of the amyloid precursor protein. J Cell Sci 2000; 113:1857-70.
5. Selkoe DJ. Alzheimer's disease: genes, proteins, and therapy. Physiol Rev 2001; 81:741-66.
6. Iwata N, Tsubuki S, Takaki Y, Watanabe K, Sekiguchi M, Hosoki E, Kawashima-Morishima M, Lee HJ, Hama E, Sekine-Aizawa Y, Saido TC. Identification of the major Abeta1-42-degrading catabolic pathway in brain parenchyma: suppression leads to biochemical and pathological deposition. Nat Med 2000; 6:143-50.
7. Turner AJ, Isaac RE, Coates D. The neprilysin (NEP) family of zinc metalloendopeptidases: genomics and function. Bioessays 2001; 23:261-9.
8. Iwata N, Tsubuki S, Takaki Y, Shirotani K, Lu B, Gerard NP, Gerard C, Hama E, Lee HJ, Saido TC. Metabolic regulation of brain Abeta by neprilysin. Science 2001; 292:1550-2.
9. Iwata N, Mizukami H, Shirotani K, Takaki Y, Muramatsu S, Lu B, Gerard NP, Gerard C, Ozawa K, Saido TC. Presynaptic localization of neprilysin contributes to efficient clearance of amyloid-beta peptide in mouse brain. J Neurosci 2004; 24:991-8.
10. Yasojima K, Akiyama H, McGeer EG, McGeer PL. Reduced neprilysin in high plaque areas of Alzheimer brain: a possible relationship to deficient degradation of beta-amyloid peptide. Neurosci Lett 2001; 297:97-100.
11. Van Broeckhoven C, Genthe AM, Vandenberghe A, Horsthemke B, Backhovens H, Raeymaekers P, Van Hul W, Wehnert A, Gheuens J, Cras P, Bruyland M, Martin JJ, Salbaum M, Multhaup G, Masters CL, Beyreuther K, Gurling HMD, Mullan MJ, Holland A, Barton A, Irving N, Williamson R, Richards SJ, Hardy JA. Failure of familial Alzheimer's disease to segregate with the A4-amyloid gene in several European families. Nature 1987; 329:153-5.
12. Tanzi RE, St George-Hyslop PH, Haines JL, Polinsky RJ, Nee L, Foncin JF, Neve RL, McClatchey AI, Conneally PM, Gusella JF. The genetic defect in familial Alzheimer's disease is not tightly linked to the amyloid beta-protein gene. Nature 1987; 329:156-7.
13. St George-Hyslop PH, Haines JL, Farrer LA, Polinsky R, Van Broeckhoven C, Goate A, McLachlan DR, Orr H, Bruni AC, Sorbi S, Rainero I, Foncin JF, Pollen D, Cantu JM, Tupler R, Voskresenskaya N, Mayeux R, Growdon J, Fried VA, Myers RH, Nee L, Backhovens H, Martin JJ, Rossor M, Owen MJ, Mullan M, Percy ME, Karlinsky H, Rich S, Heston L, Montesi M, Mortilla M, Nacmias N, Gusella JF, Hardy JA. Genetic linkage studies suggest that Alzheimer's disease is not a single homogeneous disorder. FAD Collaborative Study Group. Nature 1990; 347:194-7.
14. Wilson PW, Anderson KM, Kannel WB. Epidemiology of diabetes mellitus in the elderly. The Framingham Study. Am J Med 1986; 80:3-9.
15. Barnett AH, Eff C, Leslie RD, Pyke DA. Diabetes in identical twins. A study of 200 pairs. Diabetologia 1981; 20:87-93.
16. Newman B, Selby JV, King MC, Slemenda C, Fabsitz R, Friedman GD. Concordance for type 2 (non-insulin-dependent) diabetes mellitus in male twins. Diabetologia 1987; 30:763-8.
17. Janson J, Laedtke T, Parisi JE, O'Brien P, Petersen RC, Butler PC. Increased risk of type 2 diabetes in Alzheimer disease. Diabetes 2004; 53:474-81.
18. Moreira PI, Santos MS, Moreno AM, Seica R, Oliveira CR. Increased vulnerability of brain mitochondria in diabetic (Goto-Kakizaki) rats with aging and amyloid-beta exposure. Diabetes 2003; 52:1449-56.
19. Yoneda S, Hara H, Hirata A, Fukushima M, Inomata Y, Tanihara H. Vitreous fluid levels of beta-amyloid((1-42)) and tau in patients with retinal diseases. Jpn J Ophthalmol 2005; 49:106-8.
20. Florentin D, Sassi A, Roques BP. A highly sensitive fluorometric assay for "enkephalinase," a neutral metalloendopeptidase that releases tyrosine-glycine-glycine from enkephalins. Anal Biochem 1984; 141:62-9.
21. Dolev I, Michaelson DM. A nontransgenic mouse model shows inducible amyloid-beta (Abeta) peptide deposition and elucidates the role of apolipoprotein E in the amyloid cascade. Proc Natl Acad Sci U S A 2004; 101:13909-14.
22. Roques BP, Fournie-Zaluski MC, Soroca E, Lecomte JM, Malfroy B, Llorens C, Schwartz JC. The enkephalinase inhibitor thiorphan shows antinociceptive activity in mice. Nature 1980; 288:286-8.
23. Oh-hashi K, Nagai T, Tanaka T, Yu H, Hirata Y, Kiuchi K. Determination of hypoxic effect on neprilysin activity in human neuroblastoma SH-SY5Y cells using a novel HPLC method. Biochem Biophys Res Commun 2005; 334:380-5.
24. Johnson LV, Leitner WP, Rivest AJ, Staples MK, Radeke MJ, Anderson DH. The Alzheimer's A beta-peptide is deposited at sites of complement activation in pathologic deposits associated with aging and age-related macular degeneration. Proc Natl Acad Sci U S A 2002; 99:11830-5.
25. Dentchev T, Milam AH, Lee VM, Trojanowski JQ, Dunaief JL. Amyloid-beta is found in drusen from some age-related macular degeneration retinas, but not in drusen from normal retinas. Mol Vis 2003; 9:184-90.
26. Anderson DH, Talaga KC, Rivest AJ, Barron E, Hageman GS, Johnson LV. Characterization of beta amyloid assemblies in drusen: the deposits associated with aging and age-related macular degeneration. Exp Eye Res 2004; 78:243-56.
27. Goldstein LE, Muffat JA, Cherny RA, Moir RD, Ericsson MH, Huang X, Mavros C, Coccia JA, Faget KY, Fitch KA, Masters CL, Tanzi RE, Chylack LT Jr, Bush AI. Cytosolic beta-amyloid deposition and supranuclear cataracts in lenses from people with Alzheimer's disease. Lancet 2003; 361:1258-65.
28. Bird AC, Bressler NM, Bressler SB, Chisholm IH, Coscas G, Davis MD, de Jong PT, Klaver CC, Klein BEK, Klein R, Mitchell P, Sarks JP. Sarks SH, Soubrane G, Taylor HR, Vingerling JR. An international classification and grading system for age-related maculopathy and age-related macular degeneration. The International ARM Epidemiological Study Group. Surv Ophthalmol 1995; 39:367-74.
29. Smiddy WE, Fine SL. Prognosis of patients with bilateral macular drusen. Ophthalmology 1984; 91:271-7.

30. Wang JJ, Foran S, Smith W, Mitchell P. Risk of age-related macular degeneration in eyes with macular drusen or hyperpigmentation: the Blue Mountains Eye Study cohort. Arch Ophthalmol 2003; 121:658-63.
31. Arvanitakis Z, Wilson RS, Bienias JL, Evans DA, Bennett DA. Diabetes mellitus and risk of Alzheimer disease and decline in cognitive function. Arch Neurol 2004; 61:661-6.
32. Barber AJ, Lieth E, Khin SA, Antonetti DA, Buchanan AG, Gardner TW. Neural apoptosis in the retina during experimental and human diabetes. Early onset and effect of insulin. J Clin Invest 1998; 102:783-91.
33. Lanctot C, Fournier H, Howell S, Boileau G, Crine P. Direct targeting of neutral endopeptidase (EC 3.4.24.11) to the apical cell surface of transfected LLC-PK1 cells and unpolarized secretion of its soluble form. Biochem J 1995; 305:165-71.
34. Renneberg H, Albrecht M, Kurek R, Krause E, Lottspeich F, Aumuller G, Wilhelm B. Identification and characterization of neutral endopeptidase (EC 3. 4. 24. 11) from human prostasomes—localization in prostatic tissue and cell lines. Prostate 2001; 46:173-83.
35. Saghatelian A, Jessani N, Joseph A, Humphrey M, Cravatt BF. Activity-based probes for the proteomic profiling of metalloproteases. Proc Natl Acad Sci U S A 2004; 101:10000-5.
36. Maruyama M, Higuchi M, Takaki Y, Matsuba Y, Tanji H, Nemoto M, Tomita N, Matsui T, Iwata N, Mizukami H, Muramatsu S, Ozawa K, Saido TC, Arai H, Sasaki H. Cerebrospinal fluid neprilysin is reduced in prodromal Alzheimer's disease. Ann Neurol 2005; 57:832-42.
37. McKinnon SJ, Lehman DM, Kerrigan-Baumrind LA, Merges CA, Pease ME, Kerrigan DF, Ransom NL, Tahzib NG, Reitsamer HA, Levkovitch-Verbin H, Quigley HA, Zack DJ. Caspase activation and amyloid precursor protein cleavage in rat ocular hypertension. Invest Ophthalmol Vis Sci 2002; 43:1077-87.

The print version of this article was created on 17 Aug 2006. This reflects all typographical corrections and errata to the article through that date. Details of any changes may be found in the online version of the article.

Available online at www.sciencedirect.com
ScienceDirect
Experimental Eye Research 83 (2006) 1396–1404
EXPERIMENTAL EYE RESEARCH
www.elsevier.com/locate/yexer

Induction of matrix metalloproteinases (MMPs) and tissue inhibitors of MMPs correlates with outcome of acute experimental pseudomonal keratitis

Kousuke Ikema [a], Koki Matsumoto [a,*], Yasuya Inomata [a], Yoshihiro Komohara [b], Seiya Miyajima [a], Motohiro Takeya [b], Hidenobu Tanihara [a]

[a] *Department of Ophthalmology and Visual Science, Kumamoto University Graduate School of Medical Sciences, 1-1-1, Honjo, Kumamoto 860-0811, Japan*
[b] *Department of Cell Pathology, Kumamoto University Graduate School of Medical Sciences, 1-1-1, Honjo, Kumamoto 860-0811, Japan*

Received 25 January 2006; accepted in revised form 19 July 2006
Available online 11 September 2006

Abstract

This study aimed to investigate expressions and sources of matrix metalloproteinases (MMP)-2 and MMP-9, and of tissue inhibitors of MMP (TIMP)-1 and TIMP-2 in experimental *Pseudomonas aeruginosa* keratitis in rabbits. Pseudomonal keratitis was induced in New Zealand white rabbits, and macroscopic and microscopic examinations were performed at appropriate time points (3, 9, 12, 18, 24, 72 h). Expressions and sources of MMP-2, 9, and TIMP-1, 2 were determined using immunohistochemistry, gelatin zymography, ELISA, and RT-PCR. A typical corneal ulcer with a ring abscess was observed 12–72 h post-infection (p.i.) with *P. aeruginosa*. In microscopic examinations, massive inflammatory cell (mostly polymorphonuclear leukocytes, PMNs) infiltration and liquefactive necrosis were characteristic features. MMP-2 was constitutively expressed in keratocytes, and its expression was not apparently enhanced after pseudomonal infection as evidenced by zymography, immunostaining, and RT-PCR. However, MMP-9 and its activated form were induced, and were significantly enhanced 12–24 h p.i. MMP-9 appeared to derive from PMNs rather than from resident corneal cells. TIMP-1 was expressed in PMNs, macrophages, and keratocytes, and its expression was enhanced 72 h p.i. Although TIMP-2 was constitutively expressed as seen by immunostaining and RT-PCR, its concentration was below detection limits during the experiments. We demonstrated that MMP-9 was one of the important factors for corneal tissue destruction, because it was induced and significantly expressed in keratocytes and inflammatory cells after pseudomonal infection. Although TIMP-1 was expressed in later stages of infection, enhancement and activation of MMP-9 were much faster and stronger than those of TIMP-1, thereby facilitating tissue destruction leading to corneal ulceration.

Keywords: pseudomonal keratitis; MMP-2; MMP-9; TIMP-1; TIMP-2

1. Introduction

Keratitis caused by *Pseudomonas aeruginosa* is rapidly progressive, resistant to even vigorous treatments, and often results in corneal perforation and loss of vision (Laibson, 1972). Recently, increasing cases of pseudomonal keratitis have been observed in contact lens wearers, especially those with extended wear of soft contact lenses (Alfonso et al., 1986). Furthermore, overnight orthokeratology lens wear is another risk factor for pseudomonal keratitis (Ladage et al., 2004; Lau et al., 2003; Tabbara et al., 2000; Wang and Lim, 2003; Young et al., 2003).

Pseudomonal keratitis is characterized by corneal ulcers with a ring abscess in contrast to keratitis due to gram-positive cocci exhibiting localized abscesses (Matsumoto, 2000).

* Corresponding author. Tel.: +81 96 373 5247; fax: +81 96 373 5249.
E-mail address: matsumoto@ntthosp.jp (K. Matsumoto).

0014-4835/$ - see front matter © 2006 Elsevier Ltd. All rights reserved.
doi:10.1016/j.exer.2006.07.019

We previously reported that tissue destruction seen in *P. aeruginosa* corneal infections might result from enhanced expression of matrix metalloproteinases (MMPs) by keratocytes stimulated by exoproteases and proinflammatory cytokines, and proteolytic activation of MMPs by pseudomonal elastase (Matsumoto et al., 1992). We further reported that pseudomonal virulence factors (pseudomonal elastase, alkaline protease, and lipopolysaccharides), and inflammatory cytokines (interleukin-1β and tumor necrosis factor-α) enhanced expression of both MMP-2 and MMP-9 in cultured rabbit corneal fibroblasts (Miyajima et al., 2001). MMPs are a family of enzymes capable of degrading extracellular matrices. Most of MMPs are secreted as latent precursors, and need to be activated before performing their functions. MMP-2 and MMP-9 are independent gene products, and have unique substrate specificities. On the contrary, tissue inhibitors of MMPs (TIMPs) are major endogenous regulators of MMP activity in tissues (Opbroek et al., 1993). To date, 4 distinctive TIMPs (TIMP-1, -2, -3, and -4) have been identified. TIMP-1 binds to the inactive precursor of MMP-9, and to active forms of other MMPs (Wilhelm et al., 1989). TIMP-1 is believed to bind to the active site of MMP-2 following molecular stabilization due to binding of TIMP-2 to MMP-2 (Woessner, 1991). TIMP-2 is known to bind to MMP-2 with a 1:1 molar ratio (Goldberg et al., 1989).

This study aimed to investigate expressions and sources of MMPs (MMP-2 and MMP-9) and TIMPs (TIMP-1 and TIMP-2) in experimental pseudomonal keratitis in rabbits, to elucidate roles of these proteins in corneal ulceration.

2. Materials and methods

2.1. Animals

Female New Zealand albino rabbits ($n = 45$) weighing 1.7–2.2 kg were used in this study. Animals were housed under a well-conditioned atmosphere in the Center of Animal Resources and Development at Kumamoto University. Animals were handled and treated humanely, and experiments adhered to the Guidelines of ARVO for the use of animals. Experimental protocols were approved by the ethics committees of the University.

2.2. Preparation of bacteria and pseudomonal keratitis in rabbits

Pseudomonas aeruginosa Ueno strain, which was isolated from a patient with bilateral corneal ulcers, produces both elastase and alkaline protease. This strain was cultured in trypticase soy broth (Sigma St. Louis, Mo) for 12 h at 35 °C, with reciprocal shaking at 60 Hz. Bacteria were washed 3 times with sterile physiological saline, and concentration of the bacterial suspension was adjusted to 2×10^6 CFU/ml using a standard curve correlating viable cell numbers to optical density at 600 nm. Once rabbits were systemically anesthetized with ketamine hydrochloride and sodium pentobarbital, and topically with oxybuprocaine hydrochloride, samples of *P. aeruginosa* at 2×10^4 CFU/μl were injected into the corneal stroma in right eyes, using a 30-G needle connected to a microsyringe. Sterile physiological saline was similarly injected into the left eyes of 3 rabbits as controls.

2.3. Macroscopic observations of keratitis

Corneal lesions were macroscopically observed at appropriate times (3, 9, 12, 18, 24, and 72 h after bacterial infection), and were photographed. Observations were done in triplicates at each time point.

2.4. Histopathology and Immunohistochemistry

For histopathological examinations, enucleated eyes at appropriate times ($n = 6$ for 3, 9, 12, 18, 24, and 72 h p.i.) were fixed in 8% paraformaldehyde, and embedded in paraffin. Five-μm tissue sections were cut using a microtome, and were mounted on APS-coated micro-glass slides. Specimens were stained with hematoxylin and eosin.

For immunohistochemistry, enucleated eyes ($n = 5$ for 3, 12, 24, and 72 h p.i. and the control sample) were fixed with periodate-lysine-paraformaldehyde (PLP) fixative, and were embedded in optimal cutting temperature (O.C.T) compound. Samples were immediately frozen in liquid nitrogen, and stored at −80 °C. Six-μm frozen sections were cut from each block, and were immunostained with anti-human MMP-2, -9, TIMP-1 and -2 mouse monoclonal antibodies (DAIICHI Fine Chemical Co., Ltd, Toyama, Japan). They were visualized using diaminobenzidine (DAB) detection methods. All antibodies were diluted in PBS to the proper concentrations. Goat anti-mouse IgG antibody (Nichirei, Tokyo, Japan) was used as secondary antibody. As negative control, non-specific mouse IgG1 (Dako Cytomation, Kyoto, Japan) was used as primary antibody. Furthermore, to clarify whether macrophages expressed MMP-9, double immunostaining was performed using a specific antibody against the macrophage surface marker, RbM2. Once sections were immunostained and visualized using the DAB detection system, as described above, they were soaked in glycine for 30 min to remove non-specific binding of the secondary antibody. Then, they were washed with PBS, and were blocked with 5% goat serum. Sections were immunostained with RbM2, (mouse monoclonal antibody, Trans Genic Inc., Hyogo, Japan) and were visualized using alkaline phosphatase (AP) with BCIP/NBT (5-Bromo-4-Chloro-3-Indoxyl Phosphate/Nitro Blue Tetrazolium Chloride, DakoCytomation, Kyoto, Japan). A goat anti-mouse IgG antibody (Nichirei, Tokyo, Japan) was used as secondary antibody. Three negative controls without primary antibodies for MMP-9, RbM2, and both were also included.

2.5. Gelatin zymography

Zymography was performed using the method of Heussen and Dowdle (1980) with some modifications. Gelatin was

used as substrate at a final concentration of 0.1%. As described previously (Matsumoto et al., 1993), excised corneas were treated with 2% SDS for 1 h at room temperature, and were centrifuged at 15 000 rpm for 10 min. Supernatants were mixed with sample buffer, and were applied to a SDS PAGE gel containing the substrates. Electrophoresis was performed at 4 °C. All lanes were loaded with the same amounts of proteins. Following electrophoresis, gels were rinsed with 2.5% Triton X-100 (with or without 100 mM EDTA) for 1 h at room temperature to remove SDS. Gels were incubated in reaction buffer (50 mM Tris–HCl, pH 6.8 containing 10 mM $CaCl_2$) with or without 100 mM EDTA overnight at 37 °C. Once the gels were stained with Coomassie brilliant blue R250, proteins possessing gelatinolytic activity could be easily identified as clear lytic bands against background. Prestained standard proteins were used as molecular weight markers.

2.6. Quantification of TIMP-1 and TIMP-2

Corneal extracts obtained by homogenization and centrifugation ($n = 4$ at each time point) were added to TIMP-1 immunoassay plates (TIMP-1 ELISA kit, DAIICHI Fine Chemical Co., Ltd, Toyama, Japan) and TIMP-2 coated beads (TIMP-2 ELISA kit, DAIICHI Fine Chemical Co., Ltd, Toyama, Japan). Analysis was performed according to the manufacturer's protocols. Obtained values were revised with each corresponding sample's protein concentration. Detection limits of the systems for TIMP-1 and -2 were 51–2000 ng/ml and 20–320 ng/ml, respectively. The Fisher's method was used for statistical analysis.

2.7. Expressions and quantifications of MMP-2, -9; and TIMP-1, and -2 mRNAs

Expressions and quantifications of mRNAs for MMP-2, -9; and TIMP-1, -2 were analyzed using RT-PCR. Portions of excised corneas ($n = 4$ for each time point and control; 3, 12, 24, and 72 h p.i.) were soaked in RNA STAT-60® (TEL-TEST, INC. Los Angeles, CA), and were manually homogenized. Total RNAs were isolated according to the following procedures: chloroform was added to RNA STAT-60®, and the mixture was shaken. Homogenates were then centrifuged at 15 000 rpm for 15 min at 4 °C. The aqueous phase was transferred into a clean tube, and was mixed with isopropanol. Samples were then centrifuged at 15 000 rpm (for 10 min), and supernatants were removed. Pelleted RNA samples were washed with ethanol. RNA samples were dissolved in diethylpyrocarbonate (DEPC)-treated water. Using RNA templates obtained in this way, reverse transcription was performed to obtain complementary DNAs (cDNAs) according to the manufacturer's protocols (QIAGEN Omni script RT kit. Tokyo, Japan). RT-PCR was then performed. Primer sequences and PCR conditions for each gene studied are described in Table 1 (Berceli et al., 2004). Ten-μl samples of each PCR product were applied to a 3-% agarose gel, electrophoresed, stained with ethidium bromide, and photographed.

Furthermore, using the cDNA templates, real time PCR (Taqman PCR analysis) was performed according to the manufacturer's protocols (TaKaRa bio. Premix Ex Taq™ Tokyo, Japan). Assays were performed using the ABI PRISM® 7000 Sequence Detection System (Applied Biosystems). For MMP-2, 5′-CAAGTGGGACAAGAATCAGATCACA was used as forward primer, 5′-GAAGGCATCATCCACTGT TTCC as reverse primer and 5′-ACACGCCTGACCTCGAC as probe. For MMP-9, 5′-CCGCCAGCCCACCTT was used as forward primer, 5′-GTCGGTGAGCCTGGTTCTC as reverse primer and 5′-TCTCCTGGGAAGACCAC as probe. For TIMP-1, 5′-CTGGAACAGTCTGAGCTTCTCT was used as forward primer, 5′-CCGGCAGCGTAGGTCTT as reverse primer and 5′-AACGTTCCGGCTTCACC as probe. For TIMP-2, 5′-CCCATCAAGAGGATCCAGTATGAGA was used as forward primer, 5′-GTGTAGATGAACTCGA TGTCCTTGT as reverse primer and 5′-CAAGCAGATCAA GATGTTC as probe (Custom Taqman Gene Expression Assay Service, Applied Biosystems. Foster City, CA). The probes were labeled with a FAM dye. All quantitative PCR assays were performed in duplicates. Results were expressed as ratios of target gene mRNA copies to 18S ribosomal RNA (Applied Biosystems, Foster City, CA) copies.

3. Results

3.1. Macroscopic examinations

By 3 h after bacterial infection, no significant changes except for mild conjunctival infection compared to saline-injected control corneas (Fig. 1A) were observed (Fig. 1B). At 9 h p.i., mild corneal opacity was seen at the injection site (Fig. 1C). However, no corneal epithelial defect nor inflammatory cells in the anterior chamber was detected. Twelve to 18 h p.i., corneal ulcers with typical ring abscesses and severe chemosis were observed (Fig. 1D). Detailed observation of the anterior chamber could not be performed due to severe corneal opacity. At 24 h p.i., most of corneal ulcers extended further to perforation (Fig. 1E). The peripheral cornea showed a ground glass appearance. Anterior chamber information could not be obtained. At 72 h p.i., corneal lesions further deteriorated, and the entire cornea became opaque (Fig. 1F).

3.2. Histopathology

By 3 h p.i., no remarkable changes were observed. Apparent inflammatory cell infiltration was observed in the anterior stroma near the limbus 9–12 h p.i. (Fig. 2A). At 12 h p.i., some inflammatory cells accumulated around the injection site. At 24 h p.i., marked corneal stromal swelling with massive inflammatory cell infiltration was observed in the center of the cornea (Fig. 2B). Furthermore, liquefactive necrosis was seen inside a massive inflammatory cell infiltrated site (Fig. 2B). At higher magnification, most of inflammatory cells were identified as polymorphonuclear leukocytes (PMNs), and numerous bacteria could be seen (Fig. 2B, inset). These

Table 1
Primer sequences and amplification conditions for RT-PCR

Gene	Primer sequence	Annealing temp. (°C)	Optimal cycle	Base pair
MMP-2	AGAAGATCGACGCTGTACGAGGCTGAATACACCCAGTATTCATTG	60	35	83
MMP-9	CCGGCATTCAGGGAGATGTCGGCGTTTCCAAAGTACG	60	31	91
TIMP-1	CGCAGCGAGGAGTTTCTCACAAGTCGTGATGTGCAAGAG	55	28	62
TIMP-2	GAGATCAAGCAGATCAAGATGTTCAGGACGGCGCTGTGTAGATG	55	33	69

corneal lesions further progressed to prominent liquefactive necrosis 24–72 h p.i. (data not shown).

3.3. Immunohistochemistry

MMP-2 labeling was very faint in keratocytes in the central cornea, and around the limbus at 3 h and 12 h p.i. (data not shown). At 24 h and 72 h p.i., no remarkable labeling for MMP-2 was observed even in the central cornea where liquefactive necrosis had formed. However, significant MMP-2 staining was observed in keratocytes close to the limbus (Fig. 3A). On the other hand, MMP-9 was mainly observed in PMNs from the early phases of infection, and labeling intensity gradually increased with time. MMP-9 labeling was also observed in macrophages and keratocytes. Using double immunostaining methods, MMP-9 was detected around macrophages (Figs. 3B and C). Although MMP-9 immunostaining showed high intensity near the limbus (Fig. 3B), its intensity decreased in the central cornea, where marked liquefactive necrosis was seen 24–72 h p.i. (data not shown).

TIMP-1 was present in keratocytes and macrophages near the corneal limbus at 12–72 h p.i. (Fig. 3D). However, staining was very faint in the central cornea during the infection course (data not shown). TIMP-2 was detected in PMNs close to the limbus 12–24 h p.i. (Fig. 3E), but labeling decreased thereafter. On the contrary, around the central cornea, TIMP-2 labeling gradually increased as PMNs accumulated at the injection site 12–72 h p.i. (data not shown). All negative controls showed no detectable levels of labeling (data not shown).

3.4. Gelatin zymography

Precursor of MMP-2 (proMMP-2) was detected even in control samples (Fig. 4). In infected corneal extracts, proMMP-2 was detected 3–24 h p.i., and its activity was slightly increased at 72 h p.i. (Fig. 4). The active form was faintly detected from 12 h p.i. On the other hand, proMMP-9 and its active form were detected at 12 h p.i., and their activities significantly increased thereafter (Fig. 4). On the contrary, gels which were washed and reacted in the presence of 100 mM EDTA showed no clear lytic bands (data not shown).

3.5. Quantification of TIMP-1 and TIMP-2

TIMP-1 and TIMP-2 were quantified using an ELISA detection system kit. Concentrations of TIMP-1 at 3 and 12 h p.i. were below detection limits. Those at 24 and 72 h p.i. were 55.0 ± 8 ng/ml and 161.5 ± 33.7 ng/ml, respectively (Fig. 5). There were statistically significant differences in concentration between these 2 time points (Fisher's test, $p < 0.0001$). On the contrary, concentration of TIMP-2 was below detection limits at any time points using the ELISA kit (Fig. 5).

3.6. Expression of MMP and TIMP mRNAs

MMP-2 mRNA was detected in control and infected samples obtained at 3, 12, 24, and 72 h p.i., and its relative concentration was almost constant (Fig. 6). MMP-9 mRNA was faintly detected in control and infected samples obtained (Fig. 6) at 3 h p.i. However, its expression was clearly

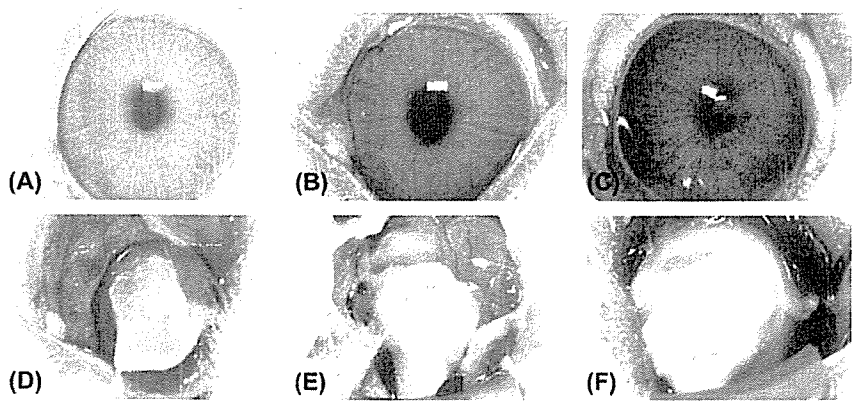

Fig. 1. Macroscopic observations of keratitis caused by *Pseudomonas aeruginosa* in rabbits. (A) Control cornea injected with saline. (B) Corneal lesion 3 h post injection (p.i.); (C) 9 h p.i.; (D) 12 h p.i.; (E) 24 h p.i.; and (F) 72 h p.i. Note that the corneal ulcer with a typical ring abscess is observed at 24–72 h p.i.

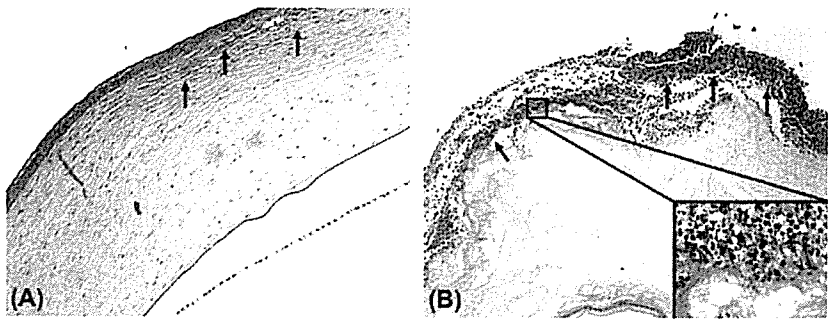

Fig. 2. Microscopic observations of keratitis caused by *P. aeruginosa*. (A) 9 h p.i. in the peripheral cornea. (×100). (B) 24 h p.i. in the central cornea (inset), higher magnification of Fig. 2B (×1000). Note the massive inflammatory cell infiltration and liquefactive necrosis. Most inflammatory cells were identified as PMNs (black arrows).

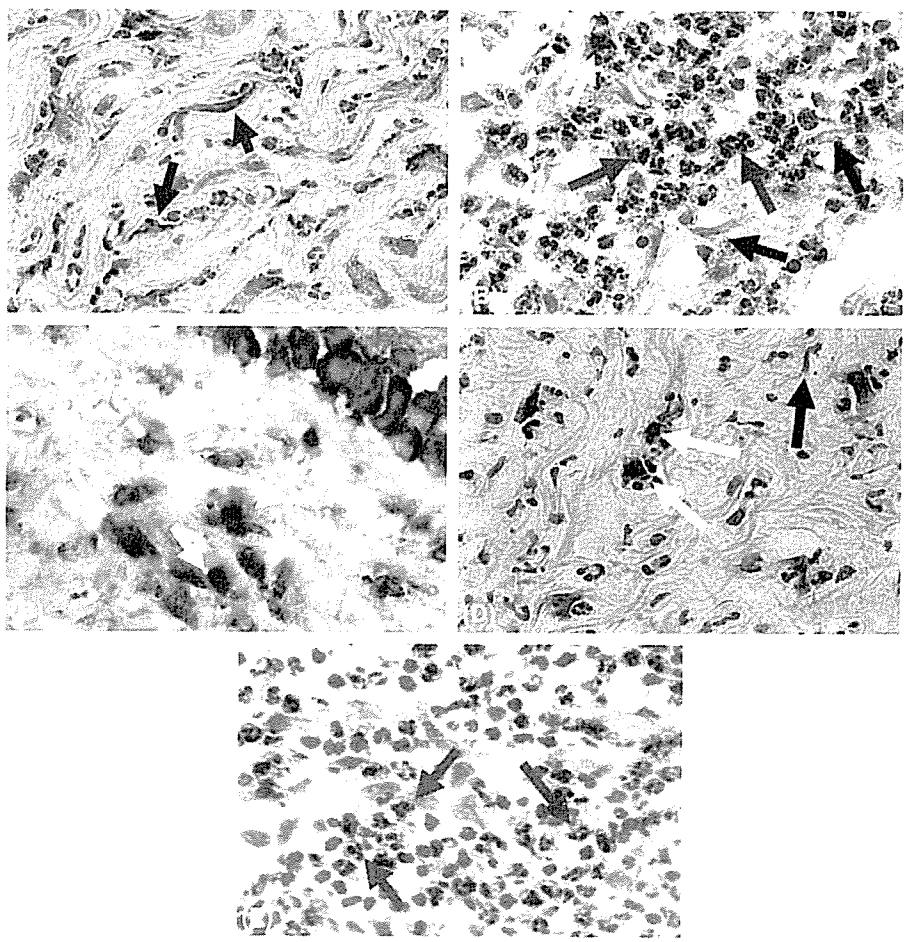

Fig. 3. Immunohistochemistry for MMPs and TIMPs. Rabbit corneal frozen sections infected with *P. aeruginosa* were immunostained with mouse monoclonal antibodies against MMP-2 and MMP-9, TIMP-1 and TIMP-2, and were visualized using a diaminobenzidine (DAB) detection system. (A) MMP-2 staining 24 h p.i. (B) MMP-9 staining 24 h p.i. (C) double immunostaining of MMP-9 24 h p.i. (×1000). (D) TIMP-1 staining 24 h p.i. (E) TIMP-2 staining 24 h p.i. All negative control specimens did not show any staining. Peripheral corneal areas are shown in the figures (original magnification, ×400). Note that MMP-2 is present exclusively in keratocytes (black arrows), whereas MMP-9 is present in inflammatory cells like PMNs (grey arrows), and macrophages (white arrows), rather than in keratocytes.

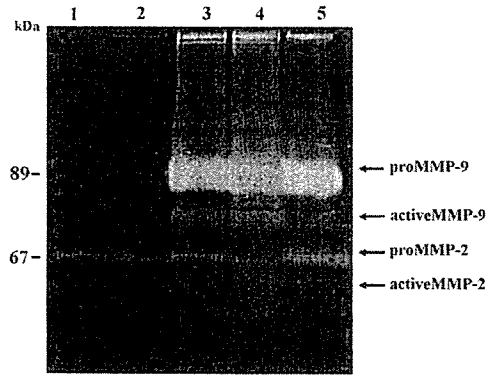

Fig. 4. Gelatin zymography. Gelatin zymography of normal corneal extracts (lane 1) or corneal extracts infected with *P. aeruginosa* obtained at 3 h (lane 2), 12 h (lane 3), 24 h (lane 4), and 72 h (lane 5). Proteins possessing gelatinolytic activity are indicated as clear lytic bands against the blue background. Note that larger amounts of gelatinolytic activity including MMP-2, MMP-9, and activated form of MMP-9 are detected in the 12-, 24-, and 72-h samples.

demonstrated at 12 h p.i., and was strongly enhanced at 24 h p.i. (Fig. 6). MMP-9 mRNA expression was then slightly reduced at 72 h p.i. Additionally, its relative concentration was also increased at 24 h p.i., and was slightly reduced at 72 h p.i. (Fig. 6). Similarly, TIMP-1 mRNA was faintly expressed at 3 and 12 h p.i., and its expression and its relative concentration significantly increased at 24 h p.i. (Fig. 6). However, its expression was somewhat reduced at 72 h p.i. Expression of TIMP-2 mRNA was detected even in control samples. Although its expression was moderate at 3–12 h p.i., it was slightly increased at 24–72 h p.i. (Fig. 6). Relative TIMP-2 mRNA concentration was increased at 72 h p.i.

4. Discussion

Our present study demonstrated that typical corneal ulcers with ring abscesses observed in rabbits by 12–24 h post-infection with a clinical isolate of *P. aeruginosa* (Fig. 1) were morphologically characterized by liquefactive necrosis, and accumulation of massive inflammatory cells, mainly PMNs (Fig. 2B). We investigated mechanisms of corneal ulceration in experimental pseudomonal keratitis in rabbits focusing on MMPs, especially MMP-2 and MMP-9, because these MMPs have been shown to be important in tissue repair, wound healing, and stromal ulceration (Fini et al., 1998).

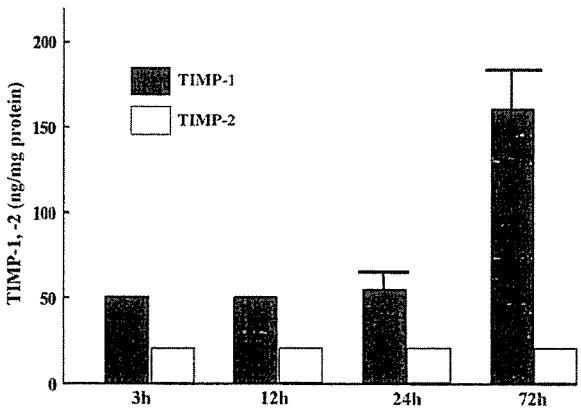

Fig. 5. Quantification of TIMP-1 and TIMP-2 concentrations using ELISA. Expressions of TIMP-1 and TIMP-2 in infected rabbit corneas were quantified using an ELISA detection kit. Results are presented as means (±standard errors) in ng/ml. Note the significant expression of TIMP-1 in the 72-h sample. On the other hand, expression of TIMP-2 was below detection limits during the experiments.

Our gelatin zymography (Fig. 4) results indicated that MMP-2 was constitutively expressed, while MMP-9 was inducible, and its expression was enhanced by pseudomonal infection. Fini et al. (1992a,b) also revealed that MMP-2 was constitutively expressed in healthy corneal cells under physiological conditions, but expression of MMP-9 was enhanced when the cornea was damaged. Moreover, Sakimoto et al. (2003) showed that even in pseudomonal keratitis with severe ulcers, active MMP-2 was not detected in the tear fluid. Matsubara et al. (1991a) suggested that MMP-2 and MMP-9 played different roles following corneal injury; namely, MMP-9 was synthesized and secreted by corneal cells with time, corresponding to a role in basement membrane degradation, whereas MMP-2 appeared during healing of corneal ulcers. Matsubara et al. (1991b) also suggested that MMP-2 performed a surveillance function in the normal cornea, catalyzing degradation of collagen molecules when the cornea was damaged. Pflugfelder et al. (2005) reported that increased MMP-9 activity on the ocular surface in response to dryness disrupted the corneal epithelial barrier function perhaps by cleaving occludins in tight junctions. Fini et al. (1991) showed that efficacy of tumor cell collagenase inhibitor in blocking progression to ulceration might be attributable to its action against MMP-9. Taken together, MMP-9 is more important than MMP-2 for tissue destruction.

Most MMPs are secreted as inactive proenzymes, and have to be cleaved and activated before performing their functions. A number of studies suggested that various factors activated MMPs. Matsumoto et al. (1992) and Matsumoto (2000) showed that secreted inactive corneal MMP-2 was activated by pseudomonal elastase. Nagano et al. (2001) suggested that pseudomonal elastase induced conversion of inactive precursors of MMP-1, -2, -3, and -9 produced by keratocytes to active forms of the enzymes. Twining et al. (1993) also demonstrated similar results. Okamoto et al. (1997) showed that purified MMP-1 (derived from human fibrosarcoma cells), MMP-8, and -9 (derived from human PMNs) were activated via limited proteolysis by bacterial proteases such as pseudomonal elastase and thermolysin. These results suggested that activated form of MMP-9 observed in our gelatin zymography was brought about via proteolytic activation by pseudomonal elastase.

Next, we investigated localizations of MMPs and TIMPs during pseudomonal infection using immunohistochemistry. Our immunostaining data for MMPs indicated that MMP-2 labeling was dependent on keratocytes while that of MMP-9 was dependent on PMN (Fig. 3A). Namely, in corneas with liquefactive necrosis, MMP-2 was detected in the limbal area rather than in the central cornea, where most keratocytes were

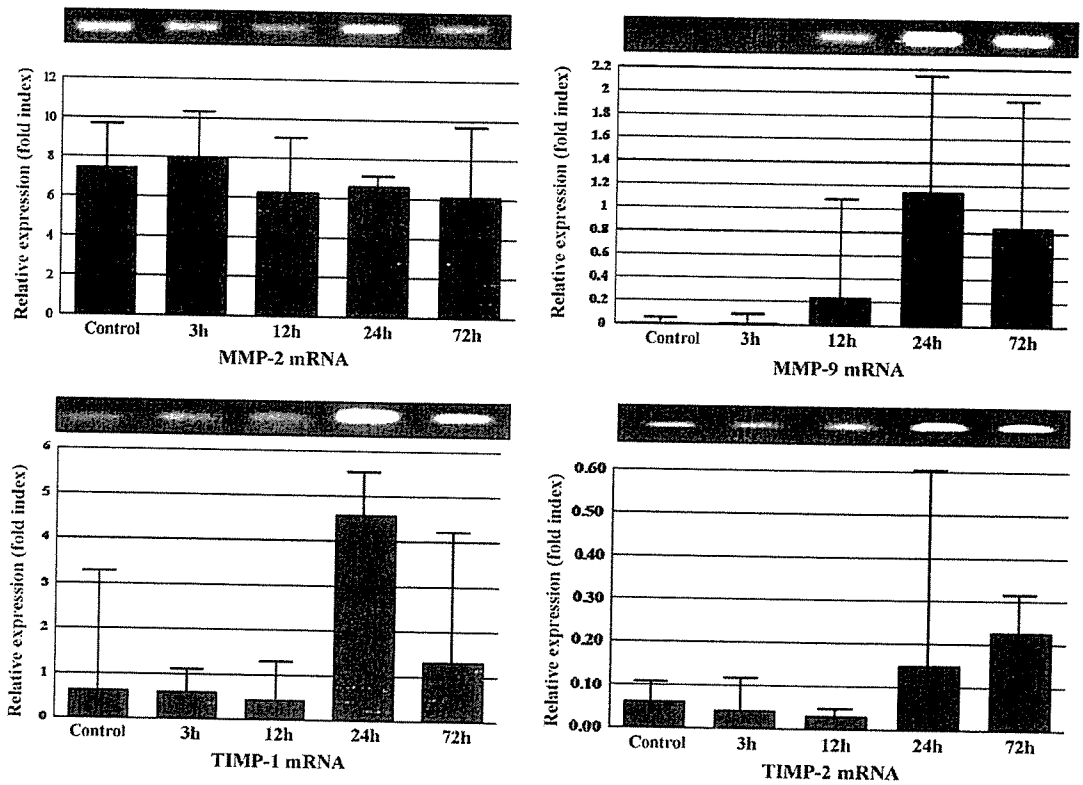

Fig. 6. Analysis of mRNAs of MMP-2, MMP-9, TIMP-1, and TIMP-2 using RT-PCR. The upper figure shows representative results of 4 independent experiments, and the lower figure shows quantitative analysis using real time PCR.

destroyed (data not shown). MMP-9 immunostaining was present in PMNs rather than in keratocytes and epithelial cells from the early stages of infection, and staining intensity gradually increased with time (Fig. 3B). However, in the later stages of infection, MMP-9 labeling was more intense in the limbal area than in the central cornea, where liquefactive necrosis was observed. We speculate that active or live PMNs exist in the limbal area, whereas dead or disrupted PMNs are present in the liquefactive necrosis area. Yang et al., 2003 showed that MMP-2 and -9 stainings were particularly intense in the proximity of ulcers, and in areas of PMN infiltration in herpetic rat keratitis models. Our findings were consistent with these notions.

Activity of MMPs is generally regulated by TIMPs. So far, 4 distinct TIMPs have been shown to exist in mammals. Balance between MMPs and TIMPs may determine net enzymatic activity in the cornea. Previous studies also demonstrated relationships between enzymes and their inhibitors (Ottinno et al., 2002). TIMP-1 is known to bind to the latent form of MMP-9. Kernacki et al. reported that TIMP-1 neutralization resulted in an overall increase in corneal MMP-9 production (Kernacki et al., 2004), and adequate endogenous expression of TIMP-1 in the cornea protected against extensive corneal tissue destruction after *P. aeruginosa* infection (Kernacki et al., 1999). Riley et al. (1995) also suggested that reduced levels of TIMP-1 expression were consistent with increased collagenase activity and tissue destruction. TIMP-1 may influence recruitment of PMNs into the infected cornea (Kernacki et al., 1999). With regards to TIMP-2, it not only acts as an inhibitor of MMP-2 by binding to MMP-2, but can also function as a co-activator of proMMP-2 (Wang et al., 2000).

Therefore, we investigated expressions and localizations of TIMP-1 and TIMP-2 in corneas after pseudomonal infection. Our immunohistochemical results demonstrated that TIMP-1 and TIMP-2 were both present in keratocytes and inflammatory cells in the area close to the limbus 12–72 h p.i. (Figs. 3C and D). However, in the central cornea where marked liquefactive necrosis was observed, intensity of TIMP-1 immunostaining was very faint during the experiments, whereas that of TIMP-2 increased with time. Immunostaining patterns for TIMP-1 and -2 agreed with previous reports (Kenney et al., 1998; Yang et al., 2003). We then quantified amounts of TIMP-1 and TIMP-2 using an ELISA detection kit. As expected, TIMP-1 concentration was enhanced at 24 and 72 h p.i., whereas that of TIMP-2 was lower than detection limits during the experiments.

In order to confirm de novo synthesis of MMPs and TIMPs, we further investigated expressions of mRNAs of MMPs and TIMPs using RT-PCR. As expected, MMP-2 mRNA was detected in control and infected corneas (Fig. 6). MMP-2 mRNA level was almost constant throughout the experiments, indicating that MMP-2 was constitutive produced (Fig. 6). On the other hand, expression of MMP-9 mRNA was significantly enhanced following pseudomonal infection (Fig. 6). These

results indicated intracorneal synthesis of MMP-9 after pseudomonal infection. From immunostaining results, it was obvious that enhanced expression of MMP-9 mRNA predominantly derived from PMNs. However, further studies are required to clarify the source of MMP-9 mRNA using in situ hybridization. With regards to TIMP-1 mRNA, its amount increased by 24 h p.i. and then decreased somewhat at 72 h p.i. (Fig. 6). On the other hand, expression of TIMP-2 mRNA was enhanced at 24 h p.i. (Fig. 6). Kernacki et al. (1998) reported that TIMP-1 mRNA was undetectable in either wounded or unwounded, non-infected corneal tissues, but increased in a time-dependent manner after corneal wounding and bacterial infection. Moreover, TIMP-2 mRNA was constitutively detected with low levels in both groups, and amounts were unchanged after corneal abrasion and bacterial inoculation. Taken together, these results indicated that TIMP-1 was inducible, and was the most important inhibitor of MMPs, especially MMP-9, in pseudomonal keratitis.

Madlener (1998) showed that both MMP-9 and TIMP-1 were strongly induced within 24 h in murine wound models. Kernacki et al. (2004) showed that adequate endogenous expression of TIMP-1 in the cornea protected the basement membrane and from stromal degradation by extensive tissue destruction via multiple processes. On the other hand, in ulcerative corneal diseases, there are lines of evidence suggesting that alterations in the ratio of MMPs vs TIMPs play a role in progressive stromal degradation. We believe that enhancement and activation of MMP-9 are much faster and stronger than those of TIMP-1, thereby facilitating tissue destruction in the cornea after pseudomonal infection. In this regard, topical application of either recombinant TIMPs or systemic MMP inhibitors would prevent or delay corneal ulceration in various disease models including pseudomonal keratitis. Furthermore, it is known that expression of MMPs is regulated by inflammatory cytokines such as IL-1β, TNF-α, and chemokines (Asano et al., 2004; Chen et al., 2004; Fini et al., 1995; Ishikawa et al., 2005; Kim et al., 2005; Xue et al., 2003). McClellan et al. (2005) reported that MMP-9 regulated immune functions in the cornea by proteolysis, potentiating *P. aeruginosa* keratitis by degrading collagen IV, and upregulating chemotactic cytokines/chemokines IL-1β and MIP-2. We are currently investigating expressions and roles of inflammatory cytokines and chemokines in pseudomonal keratitis in rabbits.

In conclusion, our present study demonstrated that MMP-9 (active form) derived mainly from PMNs was an important pathogenic factor contributing to corneal ulceration in pseudomonal keratitis.

Acknowledgments

This study was supported in part by a Grant-in-Aid for Scientific Research from the Ministry of Education, Science, Sports and Culture, Japan from the Ministry of Health and Welfare, Japan.

References

Alfonso, E., Mandelbaum, S., Fox, M.J., Forster, R.K., 1986. Ulcerative keratitis associated with contact lens wear. Am. J. Ophthalmol 101, 429–433.

Asano, K., Kanai, K.-I., Suzaki, H., 2004. Suppressive activity of fexofenandine hydrochloride on metalloproteinase production from nasal fibroblasts *in vitro*. Clin. Exp. Allergy 34, 1890–1898.

Berceli, S.A., Jiang, Z., Kingman, N.V., Pfahnl, C.L., Abouhamze, Z.S., Frase, C.D., Schultz, G.S., Ozaki, K., 2004. Differential expression and activity of matrix metalloproteinases during flow-modulated vein graft remodeling. J. Vasc. Surg 39, 1084–1090.

Chen, J., Zhang, X.M., Xiu, Q., 2004. Involvement of lymphocytes with a Th1 cytokine profile in bone cell damage associated with MMP-9 production in collagen-induced arthritis. Inflamm. Res. 53, 670–679.

Fini, M.E., Cook, J.R., Mohan, R., 1998. Proteolytic mechanisms in corneal ulceration and repair. Arch. Dermatol. Res. 290, 12–23.

Fini, M.E., Cui, T.-Y., Mouldovan, A., Grobelny, D., Galardy, R.E., Fisher, S.J., 1991. An inhibitor of the matrix metalloproteinase synthesized by rabbit corneal epithelium. Invest. Ophthalmol. Vis. Sci. 32, 2997–3001.

Fini, M.E., Girard, M.T., Matsubara, M., 1992b. Collagenolytic/gelatinolytic enzymes in corneal wound healing. Acta Ophthalmol. Suppl. 202, 26–33.

Fini, M.E., Girard, M.T., Matsubara, M., Bartlett, J.D., 1995. Unique regulation of the matrix metalloproteinase, gelatinase B. Invest. Ophthalmol. Vis. Sci. 36, 622–633.

Fini, M.E., Yue, B.Y., Sugar, J., 1992a. Collagenolytic/gelatinolytic metalloproteinases in normal and keratoconus corneas. Curr. Eye Res. 11, 849–862.

Goldberg, G.I., Marmer, B.L., Grant, G.A., Eisen, A.Z., Wilhelm, S.M., He, C., 1989. Human 72-kilodalton type IV collagenase forms a complex with a tissue inhibitor of metalloproteinases designated TIMP-2. Proc. Natl. Acad. Sci. USA 86, 8207–8211.

Heussen, C., Dowdle, E.B., 1980. Electrophoretic analysis of plasminogen activators in polyacrylamide gels containing sodium dodecyl sulfate and copolymerized substrates. Anal. Biochem 102, 196–202.

Ishikawa, T., Nishigaki, F., Miyata, S., Hirayama, Y., Minouram, K., Imanishi, J., Neya, M., Mizutani, T., Imamura, Y., Ohkubo, Y., Mutoh, S., 2005. Prevention of progressive joint destruction in adjuvant induced arthritis in rats by a novel matrix metalloproteinase inhibitor, FR217840. Eur. J. Pharmacol 508, 239–247.

Kenney, M.C., Chwa, M., Saghizadeh, M., Huang, Z.-S., Brown, D.J., 1998. Localization of TIMP-1, TIMP-2, TIMP-3, gelatinase A and gelatinase B in pathological human cornea. Curr. Eye Res. 17, 238–246.

Kernacki, K.A., Barrett, R., Hazlett, L.D., 1999. Evidence for TIMP-1 protection against *P. aeruginosa*-induced corneal ulceration and perforation. Invest. Ophthalmol. Vis. Sci. 40, 3168–3176.

Kernacki, K.A., Chunta, J.L., Barrett, R.P., Hazlett, L.D., 2004. TIMP-1 role in protection against *Pseudomonas aeruginosa*-induced corneal destruction. Exp. Eye Res. 78, 1155–1162.

Kernacki, K.A., Goebeel, D.J., Poosch, M.S., Hazlett, L.D., 1998. Early TIMP gene expression after corneal infection with *Pseudomonas aeruginosa*. Invest. Ophthalmol. Vis. Sci. 39, 331–335.

Kim, W.-J., Kang, Y.-J., Koh, E.-M., Ahn, K.-S., Cha, H.-S., Lee, W.-H., 2005. LIGHT is involved in the pathogenesis of rheumatoid arthritis by inducing the expression of pro-inflammatory cytokines and MMP-9 in macrophages. Immunology 114, 272–279.

Ladage, P.M., Yamamoto, N., Robertson, D.M., Jester, J.V., Petroll, W.M., Cavanagh, H.D., 2004. *Pseudomonas aeruginosa* corneal binding after 24-h orthokeratology lens wear. Eye Contact Lens 30, 173–178.

Laibson, P.R., 1972. Cornea and sclera. Arch. Ophthalmol 88, 553–574.

Lau, L.-I., Wu, C.-C., Lee, S.-M., Hsu, W.-M., 2003. Pseudomonas corneal ulcer related to overnight orthokeratology. Cornea 22, 262–264.

Madlener, M., 1998. Differential expression of matrix metalloproteinases and their physiological inhibitors in acute murine skin wounds. Arch. Dermatol. Res. 290, 24–29.

Matsubara, M., Girard, M.T., Kublin, C.L., Cintron, C., Fini, M.E., 1991b. Differential roles for two gelatinolytic enzymes of the matrix metalloproteinase family in the remodeling cornea. Dev. Biol. 147, 425–439.

Matsubara, M., Zieske, J.D., Fini, M.E., 1991a. Mechanism of basement membrane dissolution preceding corneal ulceration. Invest. Ophthalmol. Vis. Sci. 32, 3221–3237.

Matsumoto, K., 2000. Proteases in bacterial keratitis. Cornea 19, S160–S164.

Matsumoto, K., Shams, N.B., Hanninen, L.A., Kenyon, K.R., 1992. Proteolytic activation of corneal matrix metalloproteinases by *Pseudomonas aeruginosa* elastase. Curr. Eye Res. 11, 1105–1109.

Matsumoto, K., Shams, N.B., Hanninen, L.A., Kenyon, K.R., 1993. Cleavage and activation of corneal matrix metalloproteinases by *Pseudomonas aeruginosa* proteases. Invest. Ophthalmol. Vis. Sci. 34, 1945–1953.

McClellan, S.A., Huang, X., Barrett, R.P., Lighvani, S., Zhang, Y., Richiert, D., Hazlett, L.D., 2005. Matrix metalloproteinase-9 amplifies the immune response to *Pseudomonas aeruginosa* corneal infection. 2006. Invest. Ophthalmol. Vis. Sci. 47, 256–264.

Miyajima, S., Akaike, T., Matsumoto, K., Okamoto, T., Yoshitake, J., Hayashida, K., Negi, A., Maeda, H., 2001. Matrix metalloproteinases induction by pseudomonal virulence factors and inflammatory cytokines *in vitro*. Microb. Pathog 31, 271–281.

Nagano, T., Hao, J.-L., Nakamura, M., Kumagai, N., Abe, M., Nakazawa, T., Nishida, T., 2001. Stimulatory effect of Pseudomonal elastase on collagen degradation by cultured keratocytes. Invest. Ophthalmol. Vis. Sci. 42, 1247–1253.

Okamoto, T., Akaike, T., Suga, M., Tanase, S., Horie, H., Miyajima, S., Ando, M., Ichinose, Y., Maeda, H., 1997. Activation of human matrix metalloproteinases by various bacterial proteinases. J. Biol. Chem. 272, 6059–6066.

Opbroek, A., Kenney, M.C., Brown, D., 1993. Characterization of human corneal metalloproteinase inhibitor (TIMP-1). Curr. Eye Res. 12, 877–883.

Ottinno, P., Taheri, F., Bazan, H.E.P., 2002. Platelet-activating factor induces the gene expression of TIMP-1, -2, and PAI-1: imbalance between the gene expression of MMP-9 and TIMP-1 and -2. Exp. Eye Res. 74, 393–402.

Pflugfelder, S.C., Farley, W., Luo, L., Chen, L.Z., de Paiva, C.S., Olmos, L.C., Li, D.-Q., Fini, M.E., 2005. Matrix metalloproteinase-9 knockout confers resistance to corneal epithelial barrier disruption in experimental dry eye. Am. J. Pathol 166, 61–71.

Riley, G.P., Harrall, R.L., Watoson, P.G., Cawston, T.E., Hazleman, B.L., 1995. Collagenase (MMP-1) and TIMP-1 in destructive corneal disease associated with rheumatoid arthritis. Eye 9, 703–718.

Sakimoto, T., Shoji, J., Sawa, M., 2003. Active form of gelatinases in tear fluid in patients with corneal ulcer or ocular burn. Jpn. J. Ophthalmol 47, 423–426.

Tabbara, K.F., El-Sheikh, H.F., Aabed, B., 2000. Extended wear contact lens related bacterial keratitis. Br. J. Ophthalmol 84, 327–328.

Twining, S.S., Kirschner, S.E., Mahnke, L.A., Frank, D.W., 1993. Effect of *Pseudomonas aeruginosa* elastase, alkaline protease, and exotoxin A on corneal proteinases and proteins. Invest. Ophthalmol. Vis. Sci. 34, 2699–2712.

Wang, J.C., Lim, L., 2003. Unusual morphology in orthokeratology contact lens-related cornea ulcer. Eye Contact Lens 29, 190–192.

Wang, Z., Juttermann, R., Soloway, P.D., 2000. TIMP-2 is required for efficient activation of proMMP-2 in vivo. J. Biol. Chem. 275, 26411–26415.

Wilhelm, S.M., Collier, I.E., Marmer, B.L., Eisen, A.Z., Grant, G.A., Goldberg, G.I., 1989. SV40-transformed human lung fibroblasts secrete a 92 kDa type IV collagenase which is identical to that secreted by normal human macrophages. J. Biol. Chem. 264, 17213–17221.

Woessner, J.F., 1991. Matrix metalloproteinases and their inhibitors in connective tissue remodeling. FASEB 5, 2145–2154.

Xue, M.L., Wakefield, D., Willcox, M.D.P., Lloyd, A.R., Girolamo, N.D., Cole, N., Thakur, A., 2003. Regulation of MMPs and TIMPs by IL-1β during corneal ulceration and infection. Invest. Ophthalmol. Vis. Sci. 44, 2020–2025.

Yang, Y.-N., Bauer, D., Wasmuth, S., Steuhl, K.-P., Heiligenhaus, A., 2003. Matrix metalloproteinases (MMP-2 and 9) and tissue inhibitors of matrix metalloproteinases (TIMP-1 and 2) during the course of experimental necrotizing herpetic keratitis. Exp. Eye Res. 77, 227–237.

Young, A.L., Leung, A.T.S., Cheung, E.Y.Y., Cheng, L.L., Wong, A.K.K., Lam, D.S.C., 2003. Orthokeratology lens-related *Pseudomonas aeruginosa* infectious keratitis. Cornea 22, 265–266.

Graefe's Arch Clin Exp Ophthalmol
DOI 10.1007/s00417-006-0491-3

CASE REPORT

Loss of vision due to a physiologic pituitary enlargement during normal pregnancy

Toshihiro Inoue · Akihiro Hotta · Maiko Awai · Hidenobu Tanihara

Received: 29 May 2006 / Revised: 6 August 2006 / Accepted: 26 October 2006

Abstract
Background Physiologic pituitary enlargement during normal pregnancy is well known, but we are unaware of previous reports on a natural course of visual loss due to this disease.
Methods A 30-year-old woman presented blurred vision in the left eye from the 30th week of pregnancy. At 38 weeks visual acuity was 0.9 in the left eye. Automated perimetry revealed a mild central visual defect in the left eye. A magnetic resonance imaging (MRI) scan revealed pituitary enlargement with compression of the anterior optic chiasm. We observed the natural course of this case.
Results At 16 weeks after delivery, visual acuity was 1.5 in both eyes with normal visual field, and an MRI scan revealed a normal-sized pituitary without compression of the optic chiasm.
Conclusions Ophthalmologists should be aware of visual loss by physiologic pituitary enlargement to avoid unreasonable neurosurgical procedures.

Keywords Pituitary · Enlargement · Pregnancy · Vision

Introduction

Physiologic pituitary enlargement during normal pregnancy is well known. Magnetic resonance imaging (MRI) studies have revealed that the size of the pituitary gland increases an average of 120% during a normal pregnancy [2]. However, we are unaware of previous reports on a natural course of visual loss due to physiologic pituitary enlargement.

T. Inoue (✉) · M. Awai · H. Tanihara
Department of Ophthalmology and Visual Science,
Graduate School of Medical Sciences, Kumamoto University,
1-1-1 Honjo,
Kumamoto, Japan
e-mail: noel@da2.so-net.ne.jp

A. Hotta
Hotta Eye Clinic,
Kumamoto, Japan

Materials and methods

A 30-year-old woman presented blurred vision in the left eye from the 30th week of pregnancy. At 38 weeks she first visited our department; visual acuity was found to be 1.5 in the right eye and 0.9 in the left eye, with normal light reaction in both eyes. Automated perimetry revealed a mild central visual defect in the left eye (Fig. 1a). Slit lamp examination, intraocular pressure measurements, and funduscopy examination were normal in both eyes. An MRI scan revealed pituitary enlargement, which was 12×10×11 mm, homogeneous, and isointense, with compression of the anterior optic chiasm (Fig. 1b). The size was increased by 71.4% compared to normal pituitary size [2]. The patient did not consent to the administration of gadolinium diethylenetriaminepentaacetic (DTPA) during pregnancy. Endocrinologic studies revealed a prolactin level of 331.8 ng/ml with levels of the other pituitary hormones appropriate for gestational age. Routine chemistries were normal. Past medical history included sarcoidosis, which was stable with no medication, and one previous pregnancy, which was uncomplicated. Her family history was unremarkable. We observed the natural course of this case.

Results

At 2 weeks after delivery, an MRI scan revealed the same size of the pituitary and homogeneous enhancement of the

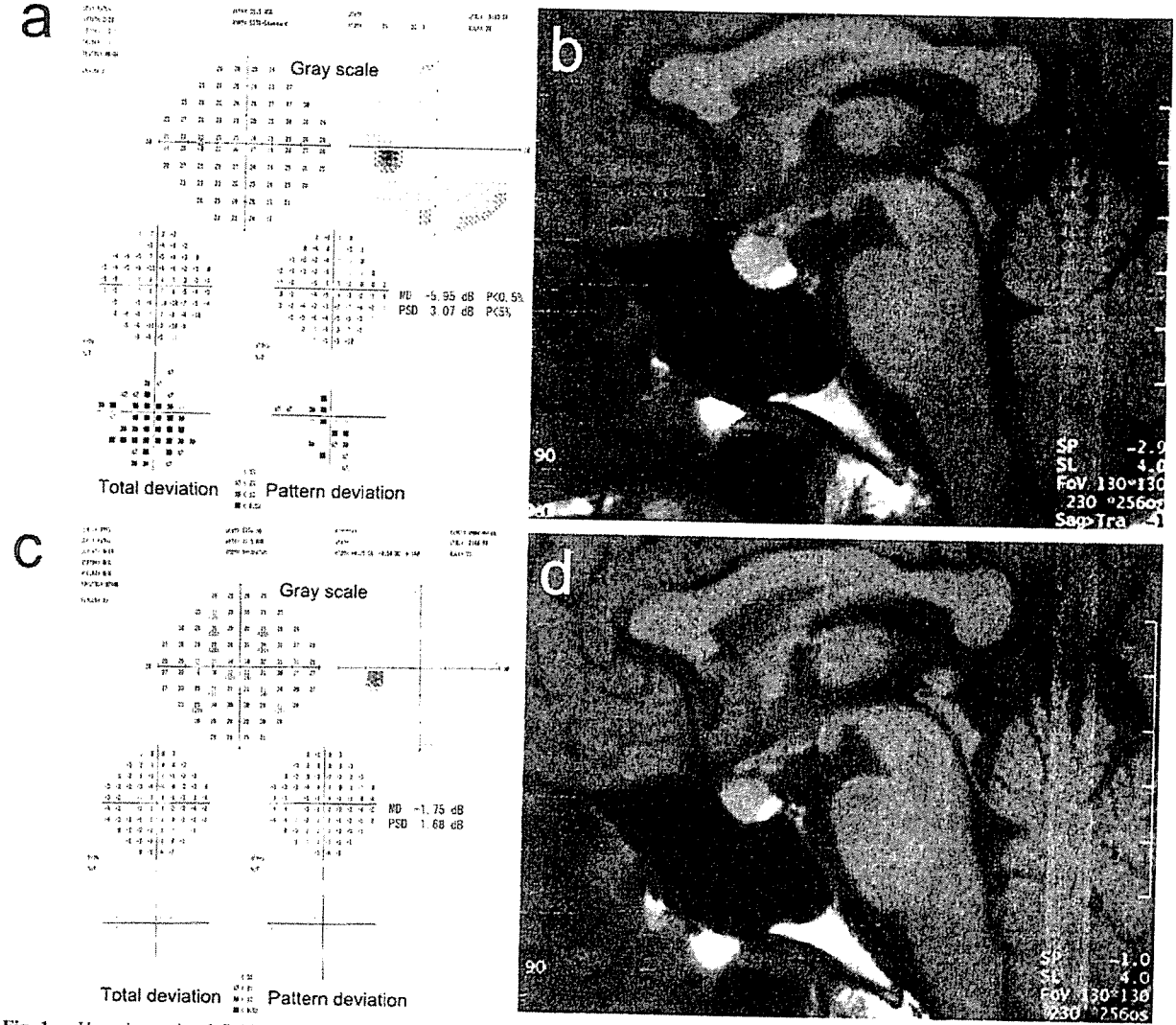

Fig. 1 **a** Humphrey visual field testing of the left eye at 38 weeks of pregnancy shows a subtle reduction in central sensitivity. **b** Sagittal view of an MRI scan of the head at 38 weeks of pregnancy, showing pituitary enlargement, which is 12×10×11 mm, homogeneous, and isointense, with compression of the anterior optic chiasm. **c** Humphrey visual field testing of the left eye at 16 weeks after delivery shows normal sensitivity. **d** Sagittal view of an MRI scan at 16 weeks after delivery, showing a normal-sized pituitary without compression of the optic chiasm

lesion after administration of gadolinium DTPA. Endocrinologic studies revealed a prolactin level of 23.1 ng/ml. At 16 weeks after delivery, visual acuity was 1.5 in both eyes with normal visual field (Fig. 1c), and an MRI scan revealed a normal-sized pituitary without compression of the optic chiasm (Fig. 1d).

Discussion

The differential diagnosis of pituitary enlargement during pregnancy is difficult because MRI is not sufficiently specific to differentiate each condition. Although prolactinoma is the most common cause of pituitary enlargement during pregnancy [3], adenoma can be ruled out in this case because of the smooth recovery after delivery. Moreover, an elevated serum prolactin level is a normal occurrence during pregnancy [4]. Considering her past medical history, granulomatous hypophysitis due to sarcoidosis was also suggested. Since this patient did not exhibit any sign of systemic sarcoid activity or show predilections for sarcoidosis, such as a lesion in the posterior pituitary gland or hypopituitarism, this seemed unlikely. Lymphocytic hypophysitis, although rare, should be suspected. Since this

condition is usually associated with autoimmune diseases [1], this was not initially considered. However, a diagnostic trial of corticosteroids should be initiated in cases with progressive visual loss after delivery, because most patients with lymphocytic hypophysitis respond well to steroids. After excluding these diseases, a clinical diagnosis of physiologic pituitary enlargement was made.

Histological examinations by a neurosurgical procedure would be needed to make a definitive diagnosis, which was not reasonable in this case because there was only mild visual loss. Although the diagnosis of this lesion is difficult, not only neurosurgeons but also ophthalmologists should be aware that physiological pituitary enlargement can cause visual loss and so should avoid unreasonable neurosurgical procedures.

Competing interests None of the authors has a proprietary interest in any products mentioned in this study.

References

1. Bellastella A, Bizzarro A, Coronella C, Bellastella G, Sinisi AA, De Bellis A (2003) Lymphocytic hypophysitis: a rare or underestimated disease? Eur J Endocrinol 149:363–376
2. Dinc H, Esen F, Demirci A, Sari A, Resit Gumele H (1998) Pituitary dimensions and volume measurements in pregnancy and post partum. MR assessment. Acta Radiol 39:64–69
3. Melmed S, Braunstein GD, Chang RJ, Becker DP (1986) Pituitary tumors secreting growth hormone and prolactin. Ann Intern Med 105:238–253
4. Soares MJ (2004) The prolactin and growth hormone families: pregnancy-specific hormones/cytokines at the maternal-fetal interface. Reprod Biol Endocrinol 2:51